# INFECTION WITH *CHLAMYDIA TRACHOMATIS* RESULTS IN DETRIMENTAL HOST CELL DEFECTS DEPENDENT UPON CELL CYCLE PROGRESSION

By

ANDREA ELIZABETH KNOWLTON

A DISSERTATION PRESENTED TO THE GRADUATE SCHOOL
OF THE UNIVERSITY OF FLORIDA IN PARTIAL FULFILLMENT
OF THE REQUIREMENTS FOR THE DEGREE OF
DOCTOR OF PHILOSOPHY

UNIVERSITY OF FLORIDA

2012

To Amy, this comes with your very own permanent marker

ACKNOWLEDGMENTS

I would like to thank my parents (all four of them) for their love, support, and encouragement. Without them none of my accomplishments thus far would have been possible; I am unbelievably lucky and forever grateful. I would like to thank my brother Ryan, and my sister Amy, for laughs, great advice, and the best family vacations.

I would like to thank my boyfriend Akio, for his support and companionship throughout graduate school, but particularly these last few months, as I am sure it is an eye-opening experience to live with a crazy person. I am very much looking forward to our next adventure together in the company of our exceptionally spoiled dog.

I would also like to thank my mentor, Dr. Scott Grieshaber for giving me the opportunity to join his lab and, to his extreme discredit, keeping me around this long. I am incredibly appreciative of all the time he has spent with me and everything I have learned. It helps to have a great project, and I have truly enjoyed this one. I would like to thank my committee members Dr. Shannon Holliday, Dr. Fred Southwick, and Dr. Shannon Wallet. I appreciate each of you taking the time out of your schedules to meet with me to discuss my progress, and your helpful advice. I would especially like to acknowledge Dr. Wallet for your help with our mouse studies, if it weren't for your advice there would be no Chapter 4.

Lastly, I want to thank the crew of the SS Grieshaber. I can honestly say I had fun, at least once, at work every day. I couldn't have gotten though this without you guys, thanks for always making me laugh.

TABLE OF CONTENTS

page

LIST OF TABLES

LIST OF FIGURES

## LIST OF ABBREVIATIONS

| | |
|---|---|
| APC | anaphase promoting complex |
| C.T. L2 | *Chlamydia trachomatis* serovar L2 |
| CDC20 | cell-division cycle protein 20 |
| CDK1 | cyclin-dependent kinase-1 |
| CIN | cervical intraepithelial neoplasia |
| CIS | carcinoma *in situ* |
| CPAF | chlamydial protease-like activity factor |
| CTXB | Cholera toxin B subunit |
| DNA | deoxyribonucleic acid |
| E | early gene |
| EB | elementary body |
| EB1 | end binding 1 |
| EDU | 5-ethynyl-2'-deoxyuridine |
| FUCCI | fluorescence ubiquitination cell cycle indicator |
| G1 | gap phase |
| G2 | second gap phase |
| GAPDH | glyceraldehyde 3-phosphate dehydrogenase |
| GCIP | Grap2 cyclin D-interacting protein |
| GFP | green fluorescent protein |
| HBSS | Hank's Balanced Salt Solution |
| HPV | human papillomavirus |
| ICC | invasive cervical carcinoma |
| IFU | inclusion forming unit |

| | |
|---|---|
| IgG | immunoglobulin G |
| K14 | keratin 14 |
| kDa | kilodalton |
| L | late protein |
| MOI | multiplicity of infection |
| MoPn | mouse pneumonitis |
| MTOC | microtubule organizing center |
| NMBD | nuclear membrane breakdown |
| NuMA | nuclear mitotic apparatus protein |
| PBS | phosphate buffered saline |
| PCM | pericentriolar material |
| PCR | polymerase chain reaction |
| Plk4 | polo-like kinase 4 |
| pRB | retinoblastoma protein |
| PV | parasitophorous vacuole |
| RB | reticulate body |
| S | synthesis phase |
| SAC | spindle assembly checkpoint |
| SCC | squamous cell carcinoma |
| SEM | standard error of the mean |
| SPG | sodium phosphate glutamate buffer |
| STI | sexually transmitted infection |
| SV40 | Simian vacuolating virus 40 |
| TARP | translocated actin-recruiting phosphoprotein |

| | |
|---|---|
| $T_F$ | transferrin |
| UV | ultraviolet |

Abstract of Dissertation Presented to the Graduate School
of the University of Florida in Partial Fulfillment of the
Requirements for the Degree of Doctor of Philosophy

# INFECTION WITH *CHLAMYDIA TRACHOMATIS* RESULTS IN DETRIMENTAL HOST CELL DEFECTS DEPENDENT UPON CELL CYCLE PROGRESSION

By

Andrea Elizabeth Knowlton

August 2012

Chair: Scott Grieshaber
Major: Medical Sciences Immunology and Microbiology

*Chlamydiae* are Gram negative, obligate intracellular bacteria, and *Chlamydia trachomatis* is the etiologic agent of the most commonly reported sexually transmitted infection (STI) in the United States. Chlamydial infections have been epidemiologically linked to increased rates in cervical cancer in patients previously infected by human papillomavirus (HPV). *Chlamydiae* undergo a biphasic life cycle that takes place inside a parasitophorous vacuole termed an inclusion. The inclusion associates very closely with host cell centrosomes, and this association is dependent upon the host motor protein dynein. We have previously reported that this interaction induces supernumerary centrosomes in infected cells, leading to multipolar mitotic spindles and inhibiting accurate chromosome segregation. Our findings demonstrate that chlamydial infection causes mitotic spindle defects independently of its effects on centrosome amplification. We show that chlamydial infection increases centrosome spread and inhibits the spindle assembly checkpoint delay to disrupt centrosome clustering. These data suggest that chlamydial infection exacerbates the consequences of centrosome amplification by inhibiting the cells' ability to suppress the effects of these defects on mitotic spindle organization. We hypothesize that these combined effects on infected dividing cells

identifies a possible mechanism for *Chlamydia* as a cofactor in cervical cancer formation. Many studies indicate that centrosome abnormalities, spindle defects, and chromosome segregation errors can lead to cell transformation. Here we demonstrate that infection with *Chlamydia trachomatis* is able to transform 3T3 cells in soft agar resulting in anchorage independence and increased colony formation. We also show for the first time *Chlamydia* infects actively replicating cells *in vivo*. Infection of mice with *Chlamydia* results in significantly increased cell proliferation within the cervix and corresponding cervical dysplasia. Confocal examination of infected tissues also revealed elements of chlamydial induced chromosome instability. These results contribute to a growing body of data implicating a role for *Chlamydia* in cervical cancer development.

# CHAPTER 1
# INTRODUCTION

## *Chlamydiae* and Host Cell Interactions

*Chlamydiae* are Gram negative, obligate intracellular bacterial organisms, with different species causing a multitude of infections in both humans and animals. *Chlamydia trachomatis* is a major human pathogen with over 15 distinct serovars that infect epithelial surfaces. Multiple urogenital serovars cause sexually transmitted infections (STI), and several ocular serovars lead to trachoma, a chronic conjunctivitis resulting in scarring and blindness (Moulder, 1991). *Chlamydia* is the most commonly reported cause of sexually transmitted infection in the United States, and the most frequent cause of preventable infectious blindness in the developing world (Cook, 2008). With a prevalence rate of about 4% among young adults and an estimated 92 million new cases worldwide each year, Chlamydia is a critical public health matter (Belland et al., 2004; Miller et al., 2004). Chlamydial infections are commonly subclinical and therefore left untreated, infections can then lead to harmful sequelae such as pelvic inflammatory disease, ectopic pregnancy, and tubal infertility (Cates and Wasserheit, 1991). Infection with *Chlamydia* has also been associated clinically with cervical metaplasia (Kiviat et al., 1985), and epidemiologically linked to an increased risk for other STIs and cervical cancer (Koskela et al., 2000; Anttila et al., 2001; Smith et al., 2002; Smith et al., 2004; Madeleine et al., 2007).

All *Chlamydiae* are obligate intracellular bacteria, and have in common a unique biphasic life cycle. The developmental cycle alternates between two distinct forms, the elementary body (EB) and the reticulate body (RB). The EB is infectious, existing as the environmentally stable and metabolically inert unit, while the RB is metabolically active,

intracellular replicative form (Moulder, 1991). The EB interacts with the host cell membrane through electrostatic interactions with heparin sulfate glycosaminoglycans and stimulates phagocytosis through a type three secretion system effector known as TARP (translocated actin-recruiting phosphoprotein), which induces actin rearrangement and internalization of the EB by the host cell (Clifton et al., 2004).The intracellular phase of the developmental cycle takes place within a membrane-bound parasitophorous vacuole termed an inclusion. The inclusion occupies a unique intracellular niche, bypassing fusion with host cell endosomal or lysosomal pathways, and intercepting exocytic vesicles containing sphingomyelin and cholesterol from the Golgi apparatus (Hackstadt et al., 1995; Carabeo et al., 2003). Once internalized EBs can begin to differentiate into RBs, and RBs replicate inside the inclusion by binary fission. After multiple rounds of replication an unknown signal induces RBs to asynchronously redifferentiate back to EB form. EBs can then initiate another round of infection allowing spread to adjacent cells (Abdelrahman and Belland, 2005).

Following de novo synthesis of chlamydial proteins the nascent inclusions are trafficked to the perinuclear region of the host cell. The inclusion is translocated along the microtubule network to the microtubule organizing center (MTOC), and this is dependent upon the minus-end directed microtubule motor protein dynein (Grieshaber et al., 2003). At the MTOC reside the host cell centrosomes and *Chlamydia* remains associated with the centrosomes throughout the developmental cycle (Grieshaber et al., 2006). *Chlamydia* is unique in that dynein is required to transport the inclusion but the dynein activating complex, dynactin, is not required; all other dynein processes employ the dynactin complex to link cargo, as well as activate dynein (Helfand et al., 2002).

Viruses and other bacterial organisms that make use of the host vesicular trafficking system, such as *Herpesviridae* or the bacterium *Orentia tsutsugamushi*, require the dynein/dynactin complex. *Chlamydia* utilizes dynein without this complex. Because chlamydial trafficking is dependent upon dynein but does not require dynactin, *Chlamydia* must initiate protein synthesis to modify the inclusion with a dynein activating complex before it can migrate to the MTOC (Grieshaber et al., 2003).

Migration of the inclusion to the MTOC is unidirectional and the inclusion remains tightly associated with the centrosomes throughout the cell cycle (Grieshaber et al., 2006). The cytoplasmic microtubule array is organized at the MTOC by the centrosomes. The centrosomes play an essential role in cell motility, organizing cellular architecture, adhesion and polarity during interphase, and nucleating bipolar spindle pole formation during mitosis (Sluder, 2004).

The centrosome consists of two centrioles embedded in an electron-dense cloud of approximately 100 proteins called the pericentriolar material (PCM). Centrioles are orthogonally positioned barrel-shaped structures that are related to the basal bodies essential for the formation of cilia and flagella. The PCM includes proteins responsible for nucleation of microtubules known as the γ-tubulin ring complex (Nigg, 2002; Andersen et al., 2003; Bettencourt-Dias and Glover, 2007). The centrosome duplication cycle is coupled with the cell cycle, with one centrosome present during G1, and then duplicated, like the chromosomes, during S-phase. During G1 the centrioles separate to become templates for the formation of new centrioles, or procentrioles, during S-phase. In S-phase the centrioles are duplicated by a semi-conservative mechanism; allowing the formation of two separate centrosomes by the beginning of G2 (Nigg, 2007). There

is a mother and a daughter centrosome for each cell after division, and the mother and daughter centrosomes migrate to opposite poles to organize the spindles for mitosis (Piel et al., 2000).

Two centrosomes are critical at mitosis for the formation of bipolar spindles; subsequent unchecked centrosome amplification leads to the formation of multipolar spindles (Fukasawa, 2007). Multipolar mitoses can result in the loss or gain of chromosomes which may lead to the eradication of tumor suppressor genes or the introduction of alleles that may promote unregulated cell growth or insensitivity to apoptotic signals (Sluder, 2004). Centrosome amplification is, therefore, a characteristic of many human cancers with defects present in low grade tumors and increasing in more aggressive carcinomas (Pihan et al., 2003). The potential role of centrosomes in cancer was first proposed by Theodore Boveri in 1914, in his book, *The Origin of Malignant Tumors*, where he proposed tumors may be the result of genetic instability as a consequence of multipolar mitoses by way of multiple centrosomes. He suggested the more abnormal mitoses a cell undergoes the more likely the cell may become malignant (Boveri, 2008). Boveri's hypothesis was ignored until several years ago; presently centrosome aberrations are widely regarded as inevitably leading to genetic instability, and that this may be a significant factor in the initiation and progression of carcinogenesis (Pihan et al., 2003; Sluder, 2004; Fukasawa, 2007; Boveri, 2008; Duensing et al., 2008).

Although centrosome amplification is clearly important for spindle multipolarity, the presence of extra centrosomes does not always lead to multipolar spindle formation. Most cell types are able to cluster extra centrosomes together during mitosis to form a

functional bipolar spindle. The coalescence of supernumerary centrosomes allows the cell to equally distribute chromosomes to avoid aneuploidy (Ring et al., 1982; Quintyne et al., 2005; Rebacz et al., 2007).

Grieshaber et al. has previously shown infection with *Chlamydia* induces supernumerary centrosomes in primary human fibroblasts, as well as aberrant spindle pole formation, and chromosome segregation defects leading to genetic instability (Grieshaber et al., 2006). The dominant interaction between the host centrosome and the chlamydial inclusion may become important in elucidating the mechanism for the increased rate in cancer formation in patients with a previous chlamydial infection (Koskela et al., 2000; Anttila et al., 2001; Smith et al., 2002; Matsumoto et al., 2003; Smith et al., 2004; Madeleine et al., 2007). It has been shown that some bacterial infections alone are able to contribute to cancer, such as *Helicobacter pylori*, but unlike viral induced cancers, bacteria lack specific oncogenes and possible molecular mechanisms to cancer are not yet clear (Lax and Thomas, 2002). While it is widely accepted that infection with human papillomavirus (HPV) is required for cervical cancer formation, HPV has been revealed to be a necessary but insufficient cause of cervical cancer. Due to a long latency period of the virus it is clear that other factors are necessary for transformation to cancer (zur Hausen, 1996). Clinically, oncogenic HPV causes transient infections of the cervix, and only a small proportion of women exposed to HPV ever progress to cervical cancer (Madeleine et al., 2007). This suggests that other cofactors are necessary in conjunction with HPV, such as other STIs, hormones, smoking, and host genetic background and immunologic responses (Ho et al., 1998)

### *Chlamydia trachomatis* and HPV Epidemiological Studies

Several studies have been completed linking *Chlamydia* as a cofactor in increased cancer rates by virtue of a past infection (Koskela et al., 2000; Anttila et al., 2001; Smith et al., 2002; Matsumoto et al., 2003; Smith et al., 2004; Madeleine et al., 2007). Koskela et al. performed large case-controlled study of 530,000 Nordic women in 2000. They examined serum samples from women diagnosed with cervical cancer and their matched controls. They then determined by microimmunofluorescence that antibodies to *Chlamydia trachomatis* were associated with an increased risk for squamous cell carcinoma (Koskela et al., 2000). Anttila et al. released a second study using serum samples from the Nordic women and confirmed similar results (Anttila et al., 2001). A case-controlled study carried out in women from Brazil and the Philippines by Smith et al. revealed women seropositive for *Chlamydia trachomatis* and positive for HPV DNA had a two-fold increase in squamous cervical cancer. This study also suggested increased serum titers correlated with increased risk for squamous cancer (Smith et al., 2002). In 2002 a population based study by Wallin et al. examined *Chlamydia trachomatis* and HPV DNA by PCR in samples from 130,000 women followed for 26 years in northern Sweden, and similarly found a prior infection with *Chlamydia* was associated with increased risk for development of invasive cervical cancer (Wallin et al., 2002). In 2004, a case-controlled study of 1200 women with invasive cervical cancer and 1100 control women from 7 different countries coordinated by the International Agency for Research on Cancer (IARC) in France corroborated the previous studies findings, confirming an overall association of *C. trachomatis* and cervical cancer while controlling for HPV DNA (Smith et al., 2004). In 2007 Madeleine et al. carried out a population based study in the Seattle-Puget Sound area determining the association of

*C. trachomatis* antibodies increased risk for squamous cervical cancer (Madeleine et al., 2007). Most recently a study of 131 women in Brazil undergoing colposcopy (microscope viewing of the cervix) or biopsy for abnormal cervical smears discovered women seropositive for *C. trachomatis* and positive for HPV DNA, specifically types 16 and 18, were at significant risk for high grade cervical neoplasia (Da Barros et al., 2012).

## Cervical Cancer

Cervical cancer is intimately linked to infection with high risk HPV types such as 16 and 18. Over 90% of squamous cell carcinomas or adenocarcinomas of the cervix are positive for integrated high risk HPV genomes 16 and 18 (zur Hausen, 1996). The HPV encoded oncoproteins E6 and E7 are consistently expressed in these cancers and a significant role in transformation to malignancy is attributed to these proteins (Münger et al., 1989).

Papillomaviruses are non-enveloped, double-stranded DNA viruses with a circular genome. They have a high species specificity and exhibit high tissue tropism for squamous epithelium. There are over 100 human papillomavirus types that have been described, and 40 of those infect the anogenital tract. It is well established that infection with certain types of HPV can cause cervical cancer, the second most common cause of cancer in women worldwide (Frazer, 2004). HPVs are classified into low- or high-risk types according to their presence in malignancies. HPV infections are associated with many other diseases such as common genital warts, and other cancers such as vulvar, vaginal, penile, anal, and oral carcinomas (zur Hausen, 2009).

The virus penetrates the epithelium through microabrasions and infects the stem cells of the basal layer that support the different epithelial layers above. HPV replication

depends on the stepwise differentiation program of these cells, therefore making culturing virus in the laboratory difficult. The virus replicates episomally in the basal stem cells, as well as in their progeny known as transit amplifying cells. The transit amplifying cells terminally differentiate to populate the suprabasal layer of the epithelium. The virus replicates in the host cell nucleus and uses the encoded early (E) genes E1 and E2 and host cellular replication machinery to replicate in the episomally maintained cells (Woodman et al., 2007). Expression of the E6 and E7 proteins delays cell cycle arrest and differentiation which is normally observed as epithelial cells move from the basement membrane to become mature keratinocytes. The delay of cell cycle arrest allows for further viral episome replication using host machinery and actually produces the thickening of the skin (wart) that is characteristic of some papillomaviruses. When the differentiation of the replicating epithelial cells to mature keratinocytes finally occurs the virus encoded structural late (L) proteins L1 and L2 are expressed and encapsidate the viral genomes in the nucleus. Mature virions are assembled in the nucleus and released from the cell as infectious particles (Narisawa-Saito and Kiyono, 2007).

Infection with high risk HPV types (16, 18, 31, 33, 35, 45, 52, and 58) can result in random integration of the viral episome into host chromosomes (Muñoz et al., 2003). Integration of the viral DNA can interrupt the negative feedback system between E2 and E6/E7 expression. E2 represses the transcription of E6 and E7 and integration of the virus leads to the disruption or loss of E2 and the subsequent overexpression of E6 and E7. As a result of this, HPV infected cells with integrated viral DNA acquire extended lifespans, preserve the ability to proliferate, and can perpetuate mutations in the

germline DNA. These cells become dysplastic which is a precursor to cervical cancer (Muñoz et al., 2006).

Oncoprotein E6 inactivates tumor suppressor and cell cycle checkpoint protein p53 by accelerating its proteolytic degradation. This can induce chromosomal instability by inhibition of p53 mediated DNA repair. Oncoprotein E7 binds and degrades pRB the retinoblastoma tumor suppressor protein, and this accounts for E7's ability to induce DNA synthesis and cellular proliferation (zur Hausen, 2009). E7 is also responsible for inducing abnormal centrosome duplication leading to spindle defects that contribute to genomic instability. E6 and E7 function synergistically, simultaneously inhibiting cellular apoptotic and anti-proliferative responses to markedly increase genetic instability (Münger and Howley, 2002).

Genital HPV infection is one of the most common sexually transmitted diseases worldwide. Approximately 20 million people in the United States are infected with HPV and another 6 million become newly infected each year. At least half of all sexually active men and women will acquire HPV at some point throughout their lives (Wheeler, 2008). In most cases infections are resolved spontaneously through an effective immune response (Narisawa-Saito and Kiyono, 2007). Understanding the role chlamydial infection plays between HPV exposure and cervical cancer incidence is important to understanding the progression of cervical cancer.

Cervical cancer arises from lesions on the cervix known as cervical intraepithelial neoplasias (CIN), which is the growth of abnormal cells in the epithelium of the cervix. CIN is not cancerous but posses the potential to progress to cancer if left unchecked by the immune system or untreated. There are three stages of CIN: CIN I, CIN II, and CIN

III, and these define how abnormal the cervical epithelial cells appear, progressing from low grade to high grade. The moderate grade CIN II and high grade CIN III can lead to severe dysplasia of the cervix followed by carcinoma in situ and finally invasive carcinoma (Wheeler, 2008).

In this study we will show chlamydial infection results in significant detriment to dividing cells. We will examine *Chlamydia's* affect on centrosome number, and positioning; the affect on spindle architecture, and resulting defect in spindle checkpoint delay and mitosis. We will present evidence for *Chlamydia's* ability to transform cells *in vitro* and provide support to this end *in vivo*. The dominant interaction between *Chlamydia* and the host cell cycle may prove to be an important step in predisposing cells to genetic instability in conjunction with HPV infection.

# CHAPTER 2
# MATERIALS AND METHODS

## Organisms and Cell Culture

*Chlamydia trachomatis* serovar L2 (LGV 434), serovar G (UW-57-Cx), and *C. muridarum* Nigg strain (referred to as mouse pneumonitis or MoPn) were grown in McCoy cells and elementary bodies (EBs) were purified by Renografin density gradient centrifugation as previously described (Howard et al., 1974). EBs were stored at -80 C until ready for use. *Coxiella burnetii* Nine Mile phase II (NMII) clone 4 was a gift from Robert Heinzen, Rocky Mountain Labs, NIAID/NIH.

All cell lines were obtained from American Type Culture Collection™. McCoy cells (CRL-1696) were maintained in DMEM (Gibco®), supplemented with 10% FBS (Cellgro®) and 10µg/mL gentamicin (Cellgro®). Neuroblastoma (N1E-115) cells (CRL-2263) were grown in RPMI-1640 (Cellgro®) supplemented with 10% fetal bovine serum (FBS) (Gibco®) and 10µg/mL gentamicin (Gibco®). HeLa 229 cells (CCL-2.1) were grown in RPMI-1640 supplemented with 10% FBS and 10µg/mL gentamicin. 3T3 (CCL-92) and COS-7 (CRL-1651) cells were maintained in RPMI-1640 medium, supplemented with 10% FBS and 10µg/mL gentamicin. End1/E6E7 (CRL-2615) cells were maintained in serum-free Keratinocyte Medium (ScienCell™) with Keratinocyte Growth Supplement (ScienCell™).

## Infection of Cultured Cells

Confluent monolayers of cells were incubated with *C. trachomatis* EBs at a MOI of approximately 5 in Hank's Balanced Salt Solution (Gibco®) for 30 minutes at room temperature while rocking. After incubation, the HBSS was removed and replaced with fresh complete media, and the infection was allowed to continue for 36 hours, unless

otherwise noted. *Coxiella burnetii* infections were carried out similarly, however cells were incubated with the inoculum for 4 hours and then replaced with fresh media containing no antibiotics. *C. burnetii* infections were allowed to continue for 96 hours.

**Immunofluorescence Staining of Cultured Cells**

Cells for fluorescent microscopy were grown on 12-mm number 1.5 borosilicate glass coverslips coated with Poly-L-lysine (Sigma®). The coverslips were either fixed in ice cold methanol for 10 minutes, or 4% paraformaldehyde for 10 minutes and permeabilized with 0.1% Triton X-100 for 15 minutes. Cultured cells were incubated with the primary antibodies as follows: mouse monoclonal anti-γ-tubulin (Sigma®), mouse monoclonal anti-β-tubulin (Sigma®), rabbit monoclonal anti-β-tubulin (Cell Signaling Technology®) and mouse monoclonal anti-dynein intermediate chain 74.1 (Covance®). *Chlamydiae* were stained with human serum from male AB plasma purchased from Sigma; specifically for Figure 3-5E, *Chlamydia trachomatis* serovar L2 was stained with a monoclonal anti-MOMP antibody, a gift from Harlan Caldwell, Rocky Mountain Labs, NIAID/NIH. To visualize the primary antibodies appropriate AlexaFluor® (Molecular Probes/Life Technologies™) conjugated secondary antibodies were used; 488/568/647 against mouse, or human immunoglobulin G (IgG). The far-red fluorescent DNA dye DRAQ5™ (Biostatus Limited) was used to visualize nuclei.

**Microscope**

Images were acquired using a spinning disk confocal system connected to a Leica DMIRB microscope with a 63x oil-immersion objective, equipped with a Photometrics cascade-cooled EMCCD camera, under the control of the Open Source software package μManager (http://www.micro-manager.org/). Images were processed using the image analysis software ImageJ (http://rsb.info.nih.gov/ij/). Representative confocal

micrographs displayed in the figures are maximal intensity projections of the 3D data sets, unless otherwise noted.

### Transfections and Plasmids

Cells were seeded on 12 mm number 1.5 glass coverslips in 24-well plates and grown to 50% confluency. Transfections were carried out using Lipofectamine 2000 (Life Technologies™) according to the manufacturer's instructions. The GFP-NuMA plasmid construct was a kind gift from Dr. Andreas Merdes, Centre National de la Recherche Scientifique-Pierre Fabre, Tolouse, France. Transfection with GFP-Plk4 was carried out as above. Human Plk4 (ATCC™) was cloned from pBlueScript into a GFP-destination vector using the Gateway® Cloning System (Life Technologies™) according to the manufacture's instructions. The GFP-EB1 plasmid was a kind gift from Dr. Jennifer S. Tirnauer, University of Connecticut Health Center.

### Nocodazole Washout

HeLa cells, neuroblastomas, or HeLas transfected with GFP-Plk4 were treated with 5μg/mL nocodazole in complete media for 30 minutes at 37°C. The cells were then washed twice with fresh media and placed at 37°C to recover. The cells were fixed at 0, 5, 10, 15, 20, and 25 minutes following the washout. The cells were subsequently stained for β-tubulin, γ-tubulin, and *Chlamydia* when necessary.

### Mitotic Index, DNA Synthesis Assays, and Stages of Mitosis Analysis

The mitotic index was calculated by determining the ratio of mitotic cells to the total number of cells present in a field of view. HeLa cells were stained with anti-phosho-Histone H3 (Thermo Scientific) to easily discern mitotic cells, and for *Chlamydia* when necessary. For the infected populations only infected cells were counted. A minimum of 1500 cells were counted over 20-30 fields and the procedure was repeated

three times. The rate of DNA synthesis in HeLa cells was determined by uptake of the thymidine analogue EdU (5-ethynyl-2'-deoxyuridine), with the use of the Click-iT® EdU kit (Life Technologies ™ C10337). For uninfected and infected populations EdU positive cells were compared with the total number of cells present in a field of view. For the infected populations only infected cells were counted. A minimum of 1500 cells were counted over 20-30 fields and the procedure was repeated three times. The stages of mitosis were determined by staining cells for DNA and establishing the number of cells in different stages of mitosis for multiple coverslips. A minimum of 200 cells were counted for each stage of mitosis for both uninfected and infected populations, and the procedure was repeated three times.

**Western Blot Analysis**

The western blot analysis for dynein localization was carried out as follows. Uninfected and infected cells were mechanically lysed in MEPS buffer {5 mM MgSO4, 5 mM EGTA, 0.25 M sucrose, 35 mM PIPES [piperazine-N,N_-bis(2-ethanesulfonic acid)]} and microtubules were stabilized with taxol, the samples were centrifuged at low and then high speeds. Each of the pellets and supernatant from the high-speed spin were run on SDS-PAGE and blotted for anti-dynein 74.1. The western blot procedure for *in vivo* cyclin B1 was carried out as follows. HeLa cells were infected with *C. trachomatis* L2 for 30 hours. Mitotic cells were shaken off the flask in PBS and centrifuged. Pellets were lysed with sample buffer (Thermo Scientific). A western blot was performed using mouse monoclonal anti-cyclin B1 (Cell Signaling Technology®) or mouse monoclonal anti-GAPDH (EnCor) followed by sheep anti-mouse HRP antibody (AbCam®). The substrate was a chemo-luminescent reagent (Pierce).

## Cell-free Degradation

Mitotic host cell proteins were collected as follows. Mitotic cells were shaken off the flask in PBS and centrifuged. Cells were lysed with NP-40 Buffer [1% NP-40, 0.5% Triton X-100, 0.15 M NaCl, 50 mM Tris pH 8.0] for 20 minutes on ice. Sample was centrifuged at 18,505 x g to remove debris and stored at -80°C. Chlamydial proteins present in the cytoplasm were collected as follows. Cells were scraped into PBS and pelleted. Cells were resuspended in douncing buffer [10 mM KCl, 1.5 mM $MgCl_2$, 1 mM ethylenediaminetetraacetic acid (EDTA), 1mM DTT, 250 mM sucrose, 20 mM Hepes-KOH pH 7.5] and dounced 5 times. Cells were centrifuged for 5 minutes at 1500 x g and the supernatant collected and further spun for 15 minutes at 100,000 x g. Supernatant was used as enzyme source. A western blot was performed as described above. Rabbit monoclonal anti-cytokeratin 8 (Abcam®) followed by goat anti-rabbit HRP antibody (Millipore) was used as a loading control.

## Immunoprecipitation

HeLa cells were lysed using Radio-Immunoprecipitation Assay (RIPA) buffer [20 mM Tris pH 7.5, 10% glycerol, 1% triton X-100, 1% deoxycholic acid, 0.1% SDS, 2.5 mM EDTA and protease inhibitor cocktail (Sigma®)] and sonicated. Cellular debris was pelleted and the supernatant was added to Protein A Agarose (Pierce) along with mouse monoclonal anti-securin (AbCam®). Following four hour room temperature incubation, the complexes were pelleted and washed [25 mM Tris pH 7.5, 150 mM NaCl, 0.1% Triton X-100]. Protein was eluted with 0.2 M glycine (pH 2.0) and neutralized with 1M Tris. Western blot analysis was performed with rabbit anti-PTTG-1 (Life Technologies™) followed by goat anti-rabbit HRP (Sigma®).

## Calculation of Dynein and NuMA in Mitotic Spindles

Three dimensional image stacks were taken and a three dimensional region of interest was drawn around the mitotic spindles and separately around the entire cell. The ratio of fluorescence intensity was calculated by dividing the fluorescence intensity in the spindle region of interest by the total intensity of the cell. N > 25, and each experiment was repeated three times.

## Calculation of Centrosome Spread

Images used for centrosome spread calculations were taken as three dimensional image stacks and maximum intensity plots were used to calculate the two dimensional spread. Because the cells are spread out on the coverslip the z dimension was very small in relation to both x and y and therefore not used in the calculation of geometric spread. The two dimensional spread was calculated using the ImageJ plug-in ‘Hull and Circle'. A region of interest was drawn around the centrosomes, which were identified by automatic thresholding of the fluorescence intensity and the area of the bounding circle was calculated from the minimal fitted polygon.

## FUCCI (Fluorescence Ubiquitination Cell Cycle Indicator)

HeLa cells were transduced with Premo™ FUCCI Cell Cycle Sensor (Life Technologies™) according to the manufacturer’s instructions. When necessary, the cells were infected with *Chlamydia* after the transduction. The cells were then imaged live for 18 hours, collecting frames every 10 minutes. For infected cells, this time period captures 24-30 hours post infection. This experiment was repeated three times each for both uninfected and infected populations. Data sets were exported to an OMERO imaging data base (http://www.openmicroscopy.org/site/products/omero). The quantification tools available in OMERO were used for the live cell intensity plots.

## Soft Agar Assay

The 3T3 soft agar transformation assay (Millipore) was performed according the manufacturer's instructions. Briefly, 3T3 cells were mock-infected, infected (*C. trachomatis* or *C. burnetii*), or treated with UV light for 1, 3, and 5 minutes. The *C. trachomatis*, and *C. burnetii* infections were cured for 3-4 days with 50µg/mL and 10µg/mL rifampicin (Fisher Scientific), respectively. The cells were allowed to recover from antibiotic treatment for 2-3 days and then plated with the appropriate controls onto minimum of four 6-well plates containing soft agar. The soft agar plates were fed with fresh media every 3-4 days, and incubated for approximately 28 days. After the incubation the cells were stained with the commercially available kit and the number of colonies per well were counted. These assays were repeated on 3-6 independent occasions.

## Mice

K14-HPV-E7 mice were obtained from Paul Lambert, McArdle Laboratory for Cancer Research, University of Wisconsin Medical School, Madison, Wisconsin, and were generated as described previously (Herber et al., 1996). The transgene was maintained in a hemizygous state on the inbred FVB/N background. All mice were housed in American Association for Accreditation of Laboratory Animal Care-approved facilities at the University of Florida, and all animal manipulations were carried out in accordance with an Institutional Animal Care and Use Committee approved protocol. University of Florida Animal Care Services provided assistance with implantation of estrogen pellets.

## Infection and Experimental Manipulation of Mice

Groups of 8-10 week old female K14-HPV-E7 mice and their wild-type littermates were injected intraperitoneally with 2.5mg Depo-Provera (Pfizer) in 100µL sterile phosphate buffered saline (PBS) at 10, and 3 days prior to infection. At 6 days prior to infection, mice were anesthetized with isoflurane and continuous release estrogen pellets delivering 0.05mg 17ß-estradiol over 60 days (Innovative Research of America) were implanted subcutaneously in the dorsal skin. The mice were then infected via the vaginal vault with $1x10^5$ inclusion-forming units (IFU) of *Chlamydia muridarum* (MoPn). Control groups for each set of mice were mock-infected with sucrose phosphate glutamate buffer [(SPG) 8mM sodium phosphate dibasic anhydrous, 2mM sodium phosphate monobasic, 220mM sucrose, 0.5mM L-glutamic acid]. Mice were sacrificed at 1 week post-infection. For three consecutive days prior to sacrifice, all groups received intraperitoneal injections of 200µg EdU (5-ethynyl-2'-deoxyuridine, Life Technologies™) in 50µL sterile PBS.

The mice represented in Figure 4-5 received no estrogen treatment and were sacrificed 5 days after initial infection. Infection was carried out as above, however infected groups were reinfected on day 3 with an additional $1x10^5$ IFU of *Chlamydia muridarum*.

## Verification of Infection

Verification of genital tract infection was adapted from the Morrison laboratory (Morrison et al., 2011), and monitored as follows. The vaginal canal was swabbed with a calcium alginate tipped swab (Fisher Scientific), and the tip was then vortexed in 500µL SPG with two sterile 4mm glass beads (Kimble Chase) for 2 minutes. Each sample was then diluted appropriately and 300µL of inoculum was placed onto McCoy

cells. The plates were centrifuged at 900 x g for 1 hour, followed by incubation at 37 C for 1 hour. After incubation the inoculum was removed and 500µL of fresh media [DMEM supplemented with 10% FBS, 15µg/mL gentamicin, and 0.25µg/mL Fungizone (amphotericin B, Life Technologies™)] was added. The infections were allowed to continue for 30 hours. The cultures were fixed with methanol and the number of IFUs was determined by indirect immunofluorescence as described above.

**Histopathology**

Whole murine reproductive tracts were harvested following sacrifice and placed in embedding cassettes (Fisher Scientific) with one sponge for compression. Reproductive tracts were fixed overnight at room temperature in 10% neutral buffered formalin (Fisher Scientific). The University of Florida Molecular Pathology Core performed paraffin-embedding, sectioning, and hematoxylin and eosin (H&E) staining of all tissues. Paraffin blocks were sectioned, with the entire organ in one plane, at 4 and 10µm as specified in the figure legends. Two H&E slides, sectioned at different depths, from each animal were evaluated by a board certified pathologist (Larry Fowler) blinded to experimental condition. Cervical intraepithelial neoplasia (CIN) scores were determined according to the published system developed with K14-HPV-E7 mice (Riley et al., 2003). The grading system ranged from 1-6 arbitrary units and assessed the nucleus:cytoplasm ratio within squamous epithelial cells, the frequency of these cells in the squamous epithelium, and the architecture of the intersection between squamous epithelium and underlying vaginal or cervical stroma. A score of 1 corresponded to normal tissue, 2 = CIN I, 3 = CIN II, 4 = CIN III, score of 5 represented carcinoma *in situ* (CIS), and squamous cell carcinoma (SCC) received a score of 6.

## Immunofluorescence Staining of Mouse Reproductive Tracts

Formalin-fixed, paraffin-embedded tissue sections were deparaffinized in two changes of xylene for 10 minutes each and then dehydrated in 100% ethanol for 5 minutes. The slides were then rehydrated through a graded ethanol series (95% and 70%) for 5 minutes each, followed by a wash in $dH_20$ for 5 minutes; all steps were carried out at room temperature. The slides were placed in sodium citrate buffer [10mM sodium citrate, 0.05% Tween 20, pH 6.0] at 96.5 C for 25 minutes. To allow the slides to cool to room temperature they were moved to a $dH_20$ bath for 5 minutes. Sections were permeabilized overnight at 4 C with 0.1% Triton X-100 (Fisher Scientific) in 1X PBS. The slides were washed in 0.5% PBS-Tween 20 (Fisher Scientific), and then blocked with 10% normal goat serum (Life Technologies™) at room temperature for a minimum of 4 hours. Slides were washed with PBST and incubated with primary antibodies diluted in 10% normal goat serum for 24 hours. Primary antibodies consisted of mouse monoclonal anti-γ-tubulin (Sigma®), and mouse monoclonal anti-E-Cadherin (BD Biosciences). *Chlamydia trachomatis* was stained with human serum from male AB plasma purchased from Sigma. Tissues were washed three times for 30 minutes each in PBST and incubated in secondary antibody for 4-8 hours. To visualize the primary antibodies appropriate AlexaFluor® (Molecular Probes/Life Technologies™) conjugated secondary antibodies were used: 488/568/647 against mouse, or human immunoglobulin G (IgG). The far-red fluorescent DNA dye DRAQ5™ (Biostatus Limited) was used to visualize nuclei.

## Calculation of Cell Proliferation

The rate of cell proliferation in mice was determined by uptake of the thymidine analog EdU (5-ethynyl-2'-deoxyuridine), with the use of the Click-iT® EdU kit per the

manufacturer's instructions (Life Technologies). Briefly, tissue sections were treated for immunofluorescence as above, however before incubation with primary antibody, the Click-iT® reaction was performed to visualize EdU positive cells. For each animal, EdU positive cells were compared with the total number of cells present in a field of view. A minimum of 2000 cells were counted over 15-20 fields, and this was completed at two different depths within the transformation zone.

### Statistical Analyses

Numerical data are presented as the mean ± SEM, unless otherwise noted, and were analyzed by the unpaired Student's t-test to compare means between two groups using GraphPad Prism® 4 software, version 4.03 for Windows (GraphPad Software, San Diego, CA).

# CHAPTER 3
# *CHLAMYDIA TRACHOMATIS* INFECTION CAUSES MITOTIC SPINDLE POLE DEFECTS INDEPENDENTLY OF ITS EFFECTS ON CENTROSOME AMPLIFICATION

## ***Chlamydia trachomatis* Inhibits Centrosome Clustering**

*Chlamydia trachomatis* infection is the leading bacterial cause of sexually transmitted infection (STI) in the United States, approaching four million cases annually (Miller et al., 2004). If left untreated, chlamydial infections can lead to more serious sequela such as pelvic inflammatory disease, ectopic pregnancy and tubal infertility (Handsfield, 1983; Guderian and Trobough, 1986; Henry-Suchet et al., 1987; Kelver and Nagamani, 1989; Reniers et al., 1989; Garland et al., 1990; Martin, 1990; Cohen and Brunham, 1999). *Chlamydia* has also been reported as a cofactor for increased cancer rates in patients previously infected by human papillomavirus (HPV) (Koskela et al., 2000; Anttila et al., 2001; Smith et al., 2002; Wallin et al., 2002; Matsumoto et al., 2003; Hinkula et al., 2004; Smith et al., 2004; Madeleine et al., 2007). At least 90% of all cervical carcinomas are associated with infection by high-risk HPV types 16 and 18 (Muñoz et al., 2003), but only a small number of women infected with HPV progress to invasive cervical cancer (ICC) (Walboomers et al., 1999). Therefore, the development of ICC depends on cofactors in conjunction with HPV, such as other STIs, hormones, smoking and host genetic background and immunologic responses.

The gain or loss of chromosomes due to mitotic defects can greatly accelerate tumor progression, and as a result, supernumerary centrosomes are seen in the carcinomas of many origins (Sluder, 2004; Saunders, 2005; Chi and Jeang, 2007). The

Reprinted with permission from Knowlton, A.E., Brown, H.M., Richards, T.S., Andreolas, L.A., Patel, R.K., and Grieshaber, S.S. (2011). Chlamydia trachomatis infection causes mitotic spindle pole defects independently from its effects on centrosome amplification. Traffic (Copenhagen, Denmark) 12, 854-66.

presence of bipolar spindles at mitosis is critical for the proper segregation of chromosomes. Failure to form bipolar spindles results in chromosome segregation errors leading to chromosome instability, and ultimately aneuploidy (Sluder, 2004). We established previously that chlamydial infection induces centrosome number defects and multipolar spindles (Grieshaber et al., 2006). Recently, Johnson et al. confirmed our findings and showed that chlamydial infection disregulates the centrosome synthesis pathway (Johnson et al., 2009). However, the presence of multiple centrosomes does not necessarily lead to mitotic spindle defects. Cells with supernumerary centrosomes have the ability to suppress multipolar spindles and undergo normal bipolar mitosis by clustering centrosomes to form only two active organizing sites (Quintyne et al., 2005; Saunders, 2005).

Clustering of centrosomes appears to require two mechanisms; organization of the microtubules by microtubule motor proteins and the spindle assembly checkpoint (SAC). The microtubule motor protein dynein along with the nuclear mitotic apparatus protein (NuMA) are proposed to focus microtubules allowing the cell to form bipolar spindles even in the presence of extra centrosomes (Merdes et al.,1996; Quintyne et al., 2005; Nguyen and Münger, 2009). The SAC, on the other hand, is a mechanism to monitor microtubule attachment to the kinetochores, delaying the onset of anaphase until the microtubules and chromosomes are properly organized (Basto et al., 2008).

In the current study, we show that chlamydial-infected cells are unable to suppress the multi-centrosome phenotype to form bipolar spindles, as cells with preexisting extra centrosomes infected with *Chlamydia* are not able to sequester these centrosomes into functional bipolar spindles. This defect in centrosome clustering is not due to

deregulation of microtubule motor proteins, as dynein and NuMA are still present in the spindles and functional, but is instead due to coordinate events of increasing centrosome spread during interphase, as well as overriding the spindle assembly checkpoint (SAC) delay. This is likely an important factor in pathogenesis especially in co-infection with HPV.

## Results

### Centrosome Defects and Spindle Defects Are Linked

We previously reported that chlamydial infection resulted in an increase in the number of cells with defective centrosome numbers as well as an increase of cells with multipolar spindles during mitosis. These two phenotypes, while functionally linked, are not mutually interdependent. It has recently become clear that eukaryotic cells have mechanisms to suppress the disruptive effects of extra centrosomes and can form normal bipolar mitotic spindles even when additional centrosomes are present (Quintyne et al., 2005). To further investigate the impact of chlamydial infection on both centrosome number defects as well as spindle pole organization defects, these phenotypes were quantitated over the time course of the chlamydial infectious cycle. The number of cells with centrosome number defects increased linearly over time before peaking at about 98% (Figure 3-1). The number of mitotic cells with spindle defects followed the same trend. The rate of increase in both centrosome number defects and spindle defects was plotted against each other resulting in a line that had a slope approaching 1 (0.76 ± 0.08; Figure 3-1A). The one-to-one linkage of these two phenotypes suggested that *Chlamydia* is inhibiting the innate centrosome clustering mechanism of mammalian cells reported by Quintyne et al. (Quintyne et al., 2005).

The linked increase in spindle pole defects with increased centrosome numbers was specific to chlamydial-infected cells. The overexpression of polo-like kinase-4 (Plk4) induces supernumerary centrosomes. Transfection of GFP-Plk4 in HeLa cells led to a dramatic increase in average centrosome numbers but did not lead to an increase in spindle defects showing that HeLa cells can actively suppress the effects of extra centrosomes (Figure 3-1C,D). These data suggest that chlamydial infection is causing spindle pole defects in addition to increasing centrosome numbers.

### Chlamydial Infection Causes Spindle Defects Independently of Centrosome Number Defects

To verify that chlamydial infection causes spindle defects independently from inducing centrosome number defects, we infected the murine neuroblastoma cell line N1E-115. This cell line has a unique phenotype in that cells possess a large number of extra centrosomes with every cell having more than two centrosomes (Quintyne et al., 2005). However, these cells have predominantly normal bipolar spindles showing an inherent ability to suppress the effects of extra centrosomes on spindle organization. We hypothesized that infection of this cell type would allow us to separate the effects of chlamydial infection on centrosome number defects from effects on spindle organization. Neuroblastomas were infected for 36 h with *C. trachomatis* serovar L2. This time point was chosen as it corresponds with a dramatic increase in both spindle pole defects and centrosome number defects, but is well before cell lysis which occurs after 48 h infection with serovar L2. Infected neuroblastoma cells had elevated centrosome numbers when compared with uninfected cells, 11.8 ± 0.5 and 9.0 ± 0.5, respectively (Figure 3-2A). However, all the cells in both infected and uninfected populations had greater than two centrosomes. To investigate the effect of chlamydial

infection on spindle pole architecture, cells were stained for microtubules and the number of metaphase cells with improperly organized mitotic spindles was quantitated. The uninfected neuroblastoma cells were able to suppress the effects of extra centrosomes as only 33.5 ± 2.9% had multipolar spindles (Figure 3-2B). However, the spindle poles of infected cells were greatly disrupted with 71.7 ± 4.1% displaying a multipolar spindle phenotype at 36 h post-infection (Figure 3-2B). This dramatic increase in defective spindles cannot be explained by the modest increase in centrosomes per cell, as the percentage of cells with intrinsic centrosome number defects (100%) did not change. This suggested that *Chlamydia* not only induces centrosome number defects but also interferes with the cells' innate ability to suppress the effects of extra centrosomes.

**Genital Serovars Also Cause Spindle Pole Defects**

The ability of a chlamydial infection to disrupt mitotic spindle organization may be an important virulence factor for *Chlamydia's* epidemiological link to cervical cancer. We asked whether the more common STI-causing serovars caused the same clustering defect. Neuroblastoma cells were infected with serovars G and L2, and with the mouse pathogen *C. muridarum*. *Chlamydia muridarum* is used as a model for human reproductive tract diseases. Infection with all the three chlamydial strains resulted in increased spindle pole defects at similar levels to that of serovar L2 (Figure 3-2).

**Centrosome Function**

The primary function of the centrosomes is to act as the minus-end anchoring and nucleating site for microtubules. There are multiple mechanisms used by cells to suppress the effects of extra centrosomes, clustering and selective suppression of centrosome activity (Brinkley, 2001). To ask whether chlamydial infection affected the

ability of the centrosome to nucleate microtubules, neuroblastoma cells were transfected with GFP-EB1. EB1 is a plus-end microtubule tracking protein and labels the growing ends of the microtubules. The centrosomes of all the EB1-transfected N1E-115 cells showed robust microtubule minus-end anchoring and nucleation, as shown by bright EB1 staining colocalizing with all centrosomes (Figure 3-3A). This staining pattern was unchanged in chlamydial-infected cells; every centrosome had equivalent amounts of EB1 fluorescence, showing that all the centrosomes in both infected and uninfected cells were functional. However, the centrosomes of the infected cells appeared to be more disorganized than in uninfected cells.

To further examine the effect of chlamydial infection on centrosome function, a nocodazole washout was performed on uninfected and infected neuroblastoma cells to test the ability of centrosomes to nucleate microtubules following depolymerization. After nocodazole treatment and subsequent recovery, the centrosomes in uninfected and infected cells were compared at 0, 5, 10, 15, 20 and 25 min. Representative images from 0 and 25-min post-washout confirm that centrosomes from both uninfected and infected cells are equally able to reestablish microtubule nucleation. At 25-min post-washout, there is a bright β-tubulin staining colocalizing with all the centrosomes (Figure 3-3B). To this end, we also performed nocodazole washouts in HeLa cells and HeLas transfected with Plk4 resulting in similar staining patterns as with the neuroblastoma cells (Figures 3-4 and 3-5).

### Chlamydial Infection Increases the Spread of Extra Centrosomes During Interphase

The physical grouping of centrosomes is a necessary step for normal bipolar mitosis. We hypothesized that chlamydial infection may affect the physical grouping of

centrosomes and that this may be a contributing mechanism to chlamydial induction of multipolar spindles.

To answer this question, we measured the geometric spread of centrosomes in infected and uninfected interphase neuroblastoma cells. The geometric spread is a measure of the area taken up by a bounding circle that encompasses the cells' centrosomes (Figure 3-6). The centrosomes in the uninfected neuroblastoma cells were clustered in an average area of 34.4 $\mu m^2$ (Figure 3-6, center box) with the middle 50% clustered between 1.5 and 24 $\mu m^2$ (Figure 3-6, box) and a fairly tight standard deviation of 69 (Figure 3-6, whiskers). This changed dramatically upon infection with *C. trachomatis* L2. The average area occupied by the geometric spread of the centrosomes was 122 $\mu m^2$ (Figure 3-6, center box), with the middle 50% spread between 10 and 164.5 $\mu m^2$ (Figure 3-6, box). The standard deviation was also much greater suggesting much more variability in the localization of the centrosomes (Figure 3-6, whiskers). This result suggests that chlamydial infection interferes with the cells' ability to localize centrosomes together in a small area; perhaps making it more difficult to physically group the centrosomes into only two active spindle poles.

**Dynein Localization and Function**

Dynein localization to the spindle poles is reported to be necessary for focusing and clustering extra centrosomes in order to form normal bipolar mitotic spindles (Quintyne et al., 2005; Nguyen et al., 2008). We previously showed that chlamydial infection causes relocalization of centrosomes from their normal cellular position and that the microtubule motor protein dynein was necessary for this effect (Grieshaber et al., 2006). We also showed that dynein is recruited and maintained on the chlamydial inclusion (Grieshaber et al., 2003). For these reasons, we hypothesized that dynein

sequestration by the chlamydial inclusion was a probable mechanism for the decrease in centrosome clustering we observed. To measure this effect, we quantified the fluorescent signal of dynein staining in the spindle poles as a percentage of the total dynein fluorescence in the entire cell including the chlamydial inclusion. If dynein was sequestered by the chlamydial inclusion, we would expect that the percentage of the dynein fluorescence signal would be reduced in the spindles. However, just the opposite was observed, in uninfected neuroblastomas 18.4% of the total dynein fluorescence signal was present in the spindle poles. The percentage of dynein fluorescence signal in chlamydial-infected cells rose to about 32.7% (Figure 3-7A,B). This finding is probably the result of an increase in the number of spindles in mitotic cells due to a chlamydial infection. Thus, sequestration of dynein by the inclusion is not likely to be involved in the induction of mitotic spindle defects. Western blot analysis showed that the total amount of dynein in the cell was unchanged (Figure 3-7C).

We next asked whether chlamydial infection affected dynein function in infected cells. Dynein is the major minus-directed motor protein complex in the cell and is responsible for the transport of a wide variety of cargo. We tested the effect of chlamydial infection on two cellular processes dependent on dynein trafficking; retrograde trafficking and trafficking to the lysosomes. Cells were infected with *C. trachomatis* L2 for 32 h and the delivery of fluorescently labeled Cholera toxin B subunit (CtxB) was measured. CtxB is delivered to the Golgi apparatus after binding to the lipid GM1 on the plasma membrane in a dynein-dependent manner. Fluorescently labeled transferrin (Tf) was used to measure dynein-dependent trafficking from the plasma membrane to the lysosome. Intensity plots demonstrate that in both chlamydial infected

and uninfected HeLa cells, Tf and CtxB are efficiently delivered from the plasma membrane to the perinuclear region by 30 min post-infection (Figure 3-7D). Normalizing the percentage of the fluorescent signal delivered over time showed that there was no delay, as the rate of delivery was not affected by chlamydial infection.

Chlamydial nascent inclusions also require dynein function for delivery to the microtubule organizing center (MTOC) of the host cell. To determine if chlamydial infection impacted nascent inclusion trafficking, we infected cells with *C. trachomatis* serovar G for 24 h followed by a 4 h infection with *C. trachomatis* serovar L2. Antibodies specific for serovar L2 were used to differentiate between the established serovar G chlamydial infection and the trafficking of the early nascent L2 inclusions. In both uninfected and serovar G-infected cells, the L2 inclusions were delivered efficiently to the MTOC of the cells with >95% of the L2 signal delivered to the perinuclear region (Figure 3-7E).

### Chlamydial Infection Does Not Alter the Recruitment of NuMA to the Mitotic Spindle

NuMA is a nuclear protein that localizes to the mitotic spindle during mitosis. In the spindle, NuMA is complexed with dynein and is required for spindle architecture. Decreased amounts of NuMA in mitotic spindles inhibit centrosome clustering and lead to multipolar spindles in many cancers (Merdes et al., 1996; Gaetz and Kapoor, 2004; Quintyne et al., 2005). We therefore, asked if chlamydial infection caused defects in NuMA localization that could potentially be a mechanism for spindle defects. To measure NuMA localization, neuroblastoma cells were transfected with a plasmid expressing GFP-tagged NuMA and the percentage of NuMA recruited to the spindles in relation to total GFP signal in the cell was calculated. In uninfected cells, 26.7% of the

GFP signal was present in the spindles and after infection with *C. trachomatis* L2 at 36 hr post-infection this increased slightly to about 28.7% of the GFP signal present in the mitotic spindles (Figure 3-8). This is consistent with the results from the dynein recruitment experiment and is probably due to chlamydial infection increasing the number of mitotic spindles.

Taken together, these experiments show that chlamydial infection does not cause multipolar spindles by inducing gross defects in the microtubule motors involved in centrosome focusing. However, chlamydial infection does lead to a disorganization of the centrosomes, likely by interfering with the local microtubule organization near the chlamydial inclusion.

**Chlamydial Infection Inhibits the Function of the SAC**

Clustering additional centrosomes to form bipolar spindles requires two mechanisms. The first is the dynein/NuMA focusing pathway which clusters extra centrosomes and nucleates the microtubules into spindles, and the second is to delay mitosis to allow time for the microtubules and centrosomes to properly organize (Basto et al., 2008). To determine if chlamydial infection affects the timing of mitosis, we measured the mitotic index and determined the stages of mitosis in infected and uninfected HeLa cells. The mitotic index is determined by calculating the ratio of cells in mitosis, as determined by the phosphorylation of Histone H3 to total interphase cells, and provides a measure of the time it takes to complete mitosis. Uninfected cells had a mitotic index of about 8.1%, whereas in infected cells the index dropped to 3.8%. To show that this drop was caused by a decrease in the time cells took to complete mitosis, we measured the frequency of cells in S phase by measuring DNA synthesis rates. The proportion of cells in S phase did not significantly change after infection with *Chlamydia*

as the percentage of 5-ethynyl-2'-deoxyuridine (EdU)-positive cells was the same between uninfected and infected cells, 61.9 ± 4.8 versus 60.6 ± 5.2, respectively (Figure 3-9A). To determine the stage of mitosis chlamydial infection was affecting, we categorized the mitotic cells. In the uninfected cell population, 7 ± 1% were in prophase, 30 ± 1% in prometaphase, 37 ± 1% in metaphase, 12 ± 1% in anaphase, and 14 ± 1% in telophase. However, in the L2-infected population there was a significant shift from metaphase to prometaphase while the other stages did not change significantly (Figure 3-9B). In the infected population, metaphase dropped to 21 ± 2% and prometaphase increased to 54 ± 3%. This shift was significantly different from the uninfected population with a p-value <0.001. The difference between prometaphase and metaphase is the organization of the chromosomes at the metaphase plate. The shift to prometaphase in the context of a lower mitotic index suggests that cells are entering anaphase before the chromosomes are completely aligned.

To verify that chlamydial-infected cells were exiting mitosis early, we measured the length of mitosis using the fluorescence ubiquitination cell cycle indicator system (FUCCI) (Sakaue-Sawano et al., 2008). HeLa cells were transduced with modified baculovirus encoding the two fluorescent proteins that respond to changes in the cell cycle. Multiple cells were imaged for 18 h using live cell microscopy. Example cells are shown (Figure 3-10A). The timing of mitosis was plotted by normalizing the start of mitosis to the first frame before nuclear membrane breakdown (NMBD) and the green fluorescent intensity (GFP-geminin) was normalized to the fluorescent signal in the nucleus at this time point. Relative signal intensity was plotted as a function of time (Figure 3-10B). Complete degradation of GFP-geminin (loss of green fluorescence) was

used as the marker for mitotic exit. The graph in Figure 3-10B represents the average time and intensity for four infected and five uninfected cells. The infected cells spent an average of 29 min less time in mitosis than the uninfected cells (53 ± 4 mins versus 82 ± 8 min, respectively; Figure 3-10C).

Taken together, these experiments show that the chlamydial-infected cells progress normally though the cell cycle but exit metaphase before the chromosomes are properly aligned. Delay of the onset of anaphase until all the chromosomes are aligned during metaphase is mediated by the SAC. Eukaryotic cells use the SAC as a safety mechanism to ensure the fidelity of chromosome segregation (Musacchio and Salmon, 2007). The SAC is switched off by the activity of the anaphase-promoting complex (APC). The APC ubiquitylates securin and cyclin B1, thereby activating the protease separase and inactivating the cyclin-dependent kinase-1 (Cdk1). Separase then cleaves cohesin complexes that hold the sister chromatids together and initiates sister-chromatid separation. Cdk1 inactivation leads to the dephosphorylation of Cdk1 substrates by protein phosphatases, and by that means enables exit from mitosis (Peters, 2006). Previous studies have indicated that chlamydial infection can lead to degradation of cyclin B1 (Balsara et al., 2006; Paschen et al., 2008). We hypothesized that the observed early onset of anaphase in chlamydial-infected cells was due to degradation of cyclin B1 and securin. To test whether cyclin B1 and securin were degraded during a chlamydial infection, mitotic cells were harvested using a mitotic shake off and the levels of cyclin B1 and securin were measured by western blot and immunoprecipitation, respectively. Securin levels were measured using immunoprecipitation, as it was present in much lower quantities than cyclin B1. In the

chlamydial-infected mitotic cells, nearly all the cyclin B1 was cleaved as a lower molecular weight band appeared and the expected 48 kDa band disappeared (Figure 3-11A). The securin immunoprecipitation experiments demonstrated that securin was also degraded in the chlamydial-infected cells. GAPDH was used as a loading control (Figure 3-11B).

Cyclin B1 is cleaved by a chlamydial protease-like activity factor (CPAF) secreted into the cytosol of infected cells (Balsara et al., 2006; Paschen et al., 2008). To determine if securin was similarly cleaved by a secreted protease, we purified the cytosolic fraction from infected cells using the method reported for CPAF purification (Zhong et al., 2001). The cytosolic fraction was incubated with mitotic host proteins and a western blot was performed to analyze the degradation. Cyclin B1 and securin were both cleaved after incubation with infected cytosolic lysate and compared with keratin 8 as a control (Figure 3-11C). In the immunoprecipitation experiments we observed complete disappearance of the securin signal, whereas in the cell-free degradation assay we observed cleavage of the protein. We believe this is because we precipitate with a C-terminally targeted antibody and attempted detection with an N-terminally target antibody.

## Discussion

In previous studies, we showed that the chlamydial inclusion acquires the dynein motor protein and initiates migration from the cell periphery to the MTOC early after entry (Grieshaber et al., 2003). The interaction between dynein and the chlamydial inclusion continues throughout the chlamydial life cycle (Grieshaber et al., 2006). This association results in centrosome number defects and centrosome mislocalization (Grieshaber et al., 2006). Recently, Johnson et al. confirmed centrosome amplification

and showed that chlamydial infection disregulates centrosome duplication (Johnson et al., 2009). We have also shown that infected cells display an increased frequency of multipolar mitotic spindles(Grieshaber et al., 2006). Multipolar spindles are found in many cancers and lead to an increase in chromosome instability that can be an important step in cellular transformation. The mechanisms that regulate spindle bipolarity and organization are not completely understood. However, centrosome number defects play a necessary role in this process. Supernumerary centrosomes provide extra nucleation sites for the formation of aberrant spindles. Extra centrosomes do not always lead to multipolar spindles as eukaryotic cells have multiple mechanisms to suppress the effects of too many centrosomes.

In this study, we showed that chlamydial infection causes spindle defects during mitosis independently of its effect on centrosome amplification. Proper spindle formation in the presence of extra centrosomes requires at least two major cellular functions; centrosome clustering and a delay in mitosis for the clustering-focusing pathway to successfully form only two spindle poles. The centrosome clustering and spindle-focusing pathway require localization of both dynein and the NuMA protein in the mitotic spindles (Merdes et al., 1996; Quintyne et al., 2005). We were surprised to find that chlamydial infection did not measurably affect the recruitment of either of these proteins to the mitotic spindle, or did infection affect diverse dynein functions within the cell. We initially hypothesized that, like the mechanism in many cancer cells, sequestration of dynein by the chlamydial inclusion would lead to a loss of dynein and NuMA in the spindles and would be a likely mechanism for the disruption of centrosome clustering (Merdes et al., 1996; Quintyne et al., 2005). Instead, it appears that infection with

*Chlamydia* induces spindle defects by disrupting centrosome organization during interphase and inhibiting mitotic arrest.

Chlamydial infection of cells (cell line N1E-115) with inherent centrosome number defects resulted in an increase in the spread of the supernumerary centrosomes. This result is probably mediated by the same mechanism that leads to displacement of the centrosomes from their normal juxtanuclear position in cells with normal centrosome numbers (Grieshaber et al., 2006). We have previously shown that the centrosomes interact directly with the chlamydial inclusion and that this interaction is mediated by dynein (Grieshaber et al., 2006). We believe that the increase in the spread of supernumerary centrosomes caused by chlamydial infection is the result of a direct cis-interaction between the chlamydial inclusion and centrosomes mediated by dynein. This spread is likely due to a direct interaction with the chlamydial inclusion prohibiting normal centrosome movement.

Chlamydial infection significantly decreased the mitotic index of infected cells but did not change the rate of S phase in the cell cycle. Other labs have also reported that chlamydial infection does not significantly change the length of the cell cycle (Campbell et al., 1989; Greene and Zhong, 2003; Greene et al., 2004). Infection also leads to a shift in the mitotic cells of the infected population from metaphase to prometaphase. These data suggest that infected cells are spending less time in mitosis and prematurely transitioning from metaphase to anaphase, indicating that infection inhibits the function of the SAC. The SAC acts to arrest mitosis, giving the spindles and the chromosomes time to properly attach and align at the metaphase plate. It is triggered by unattached kinetochores and lack of tension between sister chromatids (Musacchio and

Salmon, 2007). The SAC arrests mitosis by negatively regulating cdc20 activation of the APC which mediates polyubiquitylation of cyclin B1 and securin (Musacchio and Salmon, 2007). It is the inhibition of the degradation of these two proteins that keeps the cell from progressing to anaphase (Musacchio and Salmon, 2007). We show here that chlamydial infection actively overrides cell cycle arrest by causing the degradation of the two targets of the APC; cyclin B1 and securin. We do not yet know what chlamydial factor(s) are involved in the cleavage of securin but it is likely that the chlamydial effector CPAF is involved as it has been shown to target cyclin B1 (Balsara et al., 2006; Paschen et al., 2008). Other factors may also contribute to chlamydial regulation of the cell cycle. For example, the type III secretion effector CT847 is reported to interact with the host cellular Grap2 cyclin D-interacting protein (GCIP) and is proposed to drive chlamydial-infected cells through the G1/S cell cycle checkpoint (Chellas-Géry et al., 2007).

Taken together, these data in combination with the data from Johnson et al. support the idea that chlamydial infection actively promotes spindle defects and chromosome instability by affecting at least three independent cellular pathways, disregulation of centrosome duplication (Johnson et. al.), capture of centrosomes through dynein resulting in mislocalization of centrosomes (this study) and lastly, overriding the SAC-driving infected cells through mitosis in the presence of spindle defects and unaligned chromosomes.

The role that disregulation of the SAC plays in the chlamydial infectious cycle is not clear, as most of the cells infected by a natural chlamydial infection are terminally differentiated. However, one class of cells that would be impacted by the inhibition of

cell cycle checkpoints leading to increased spindle defects are cells coinfected with HPV. We hypothesize that the combined effects of centrosome number defects, increases in centrosome spread, and inhibition of the SAC and other cell cycle checkpoints may contribute to cervical cancer in patients previously infected with HPV.

Figure 3-1. Centrosome abnormalities correlate with spindle dysfunction. A) HeLa cells were infected with *Chlamydia trachomatis* serovar L2, and fixed at 0, 24, 32, and 48 hours post-infection. Cells were stained with anti-γ-tubulin for centrosomes (green), anti-β-tubulin for spindle poles (red), and with human serum for *Chlamydia* (blue). The percentage of infected cells with greater than two centrosomes and greater than two spindle poles were counted for each time point (mock-infected cells were counted for the 0 hr time point). A linear regression model generated a positive slope of 0.76 ± 0.1, and $r^2$=0.97. B) Representative confocal micrograph, displaying an infected multipolar cell, and an uninfected bipolar cell. C) HeLa cells were transfected with GFP-Plk4. Centrosomes (arrows) were stained with anti-γ-tubulin (green), centrosomes from transfected populations were easily identified as GFP positive. The uninfected cells were co-stained for DNA (blue), the infected cells were co-stained for *Chlamydia* (red). The GFP-Plk4 transfected cells were co-stained for microtubules (red) and DNA (blue). The cells were counted for both uninfected and infected populations resulting in 2.2 ± 0.1 average centrosomes per cell, and increasing to 3.2 ± 0.3 average centrosomes/cell 36 hours post-infection. The Plk4 transfected cells were counted for GFP positive centrosomes and this population contained 3.7 ± 0.2 average centrosomes/cell, n > 150 for each population. D) Spindle poles (arrows) were stained with anti-β-tubulin and quantitated by counting the percentage of cells with more than two spindle poles in the uninfected, infected, and GFP-Plk4 transfected populations resulting in 5.5 ± 0.8 48.3 ± 3.4, and 5.0 ± 4.0 percent multipolar spindles, respectively. The percentage of cells with multipolar spindles is significantly higher in infected cells compared to Plk4 positive cells, p=0.0012 (Student's t-test) n > 100 for each population. The representative confocal micrographs are co-stained as above, with the exception of the infected cell, in which *Chlamydia* is also stained with the DNA dye DRAQ5™. Scale bars, 5μm.

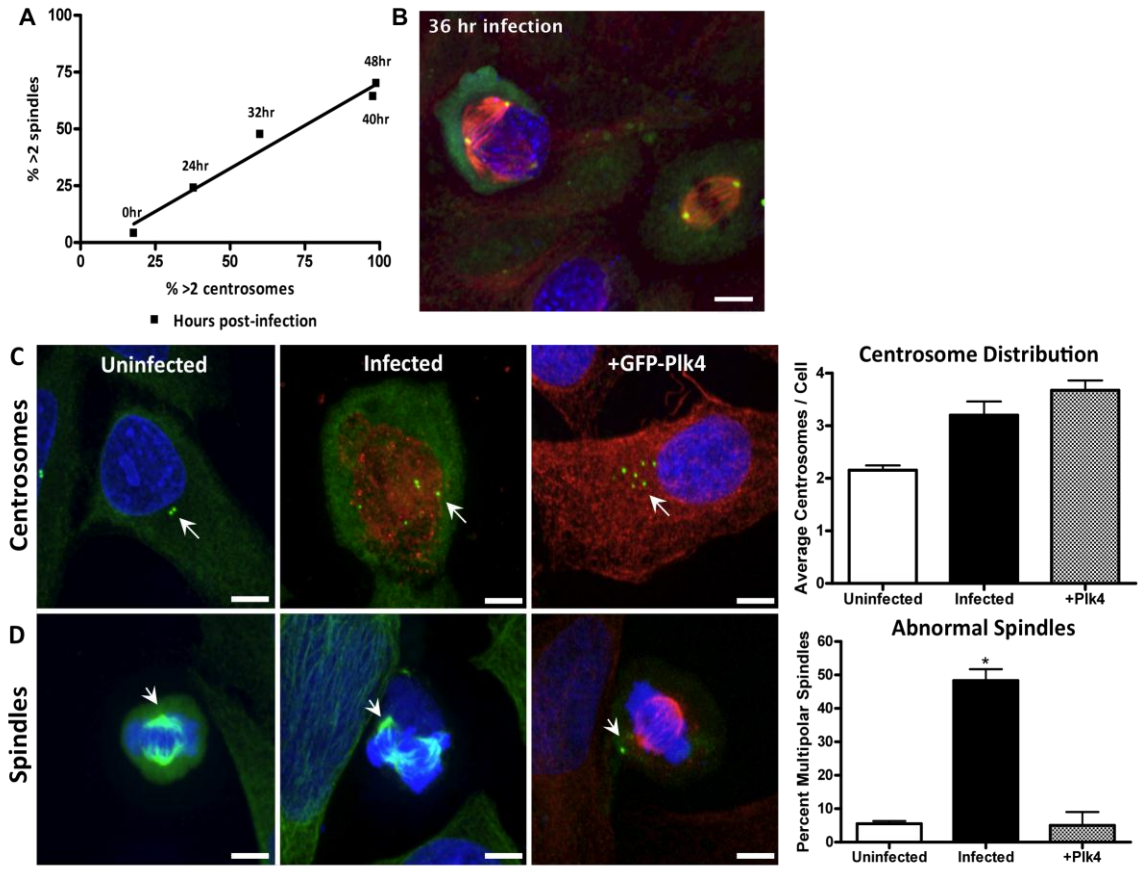
A
100
75
50
25
0
% >2 spindles
0hr
24hr
32hr
48hr
40hr
0
25
50
75
100
% >2 centrosomes
Hours post-infection
B
36 hr infection
C
Centrosomes
Uninfected
Infected
+GFP-Plk4
Centrosome Distribution
Average Centrosomes / Cell
4
3
2
1
0
Uninfected
Infected
+Plk4
D
Spindles
Abnormal Spindles
Percent Multipolar Spindles
60
50
40
30
20
10
0
*
Uninfected
Infected
+Plk4

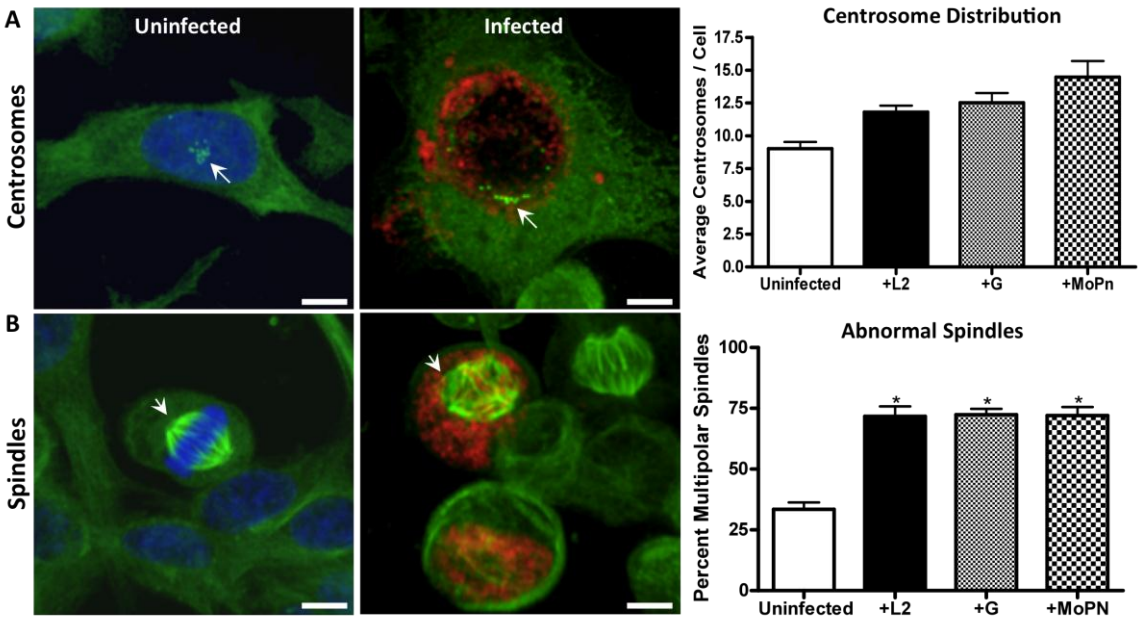


Figure 3-2. Chlamydial infection induces slight centrosome amplification, but significant spindle defects in neuroblastomas. A) Uninfected neuroblastomas were stained with anti-γ-tubulin for centrosomes (green), and DNA (blue). Neuroblastomas were infected with serovars L2, G, and *Chlamydia muridarum* (MoPn) and then stained for centrosomes (green), and *Chlamydia* (red). The cells were imaged, and the centrosomes (arrows) were then counted for each population, n > 150. The uninfected cells averaged 9 ± 0.5 centrosomes/cell, and the infected cells averaged 11.8 ± 0.5, 12.5 ± 0.7, and 14.5 ± 1.2 centrosomes/cell, respectively. B) For spindle pole quantification uninfected neuroblastomas were stained with anti-β-tubulin for spindle poles (green), and DRAQ5™ (blue). Infected neuroblastomas were stained for spindles (green) and for *Chlamydia* (red). Mitotic cells were counted for each population (arrows), n > 100. The infected population is 71.7 ± 4, 72.3 ± 2.4, and 72.1 ± 3.4 percent multipolar, respectively, compared to 33.5 ± 2.9 percent multipolar in uninfected controls. *p < 0.0015 (Student's t-test). Scale bars, 5μm.

Figure 3-3. Centrosome function is not inhibited by chlamydial infection. A) Uninfected and infected neuroblastomas were transfected with GFP-EB1 (green), a plus-end microtubule tip- tracking protein. The cells were subsequently stained for centrosomes (red), and *Chlamydia* (blue) as necessary. The cells were imaged by confocal microscopy to evaluate the function of the centrosomes after infection. B) Neuroblastomas were incubated with nocodazole and allowed to recover. The cells were fixed and stained at sequential time points during recovery for centrosomes (green), microtubules (red), and *Chlamydia* (blue) as necessary. The panels at time zero exhibit confocal images of cells at the time of washout. The panels at 25 minutes display cells that have been allowed to recover for 25 minutes after washout. Scale bars, 5μm.

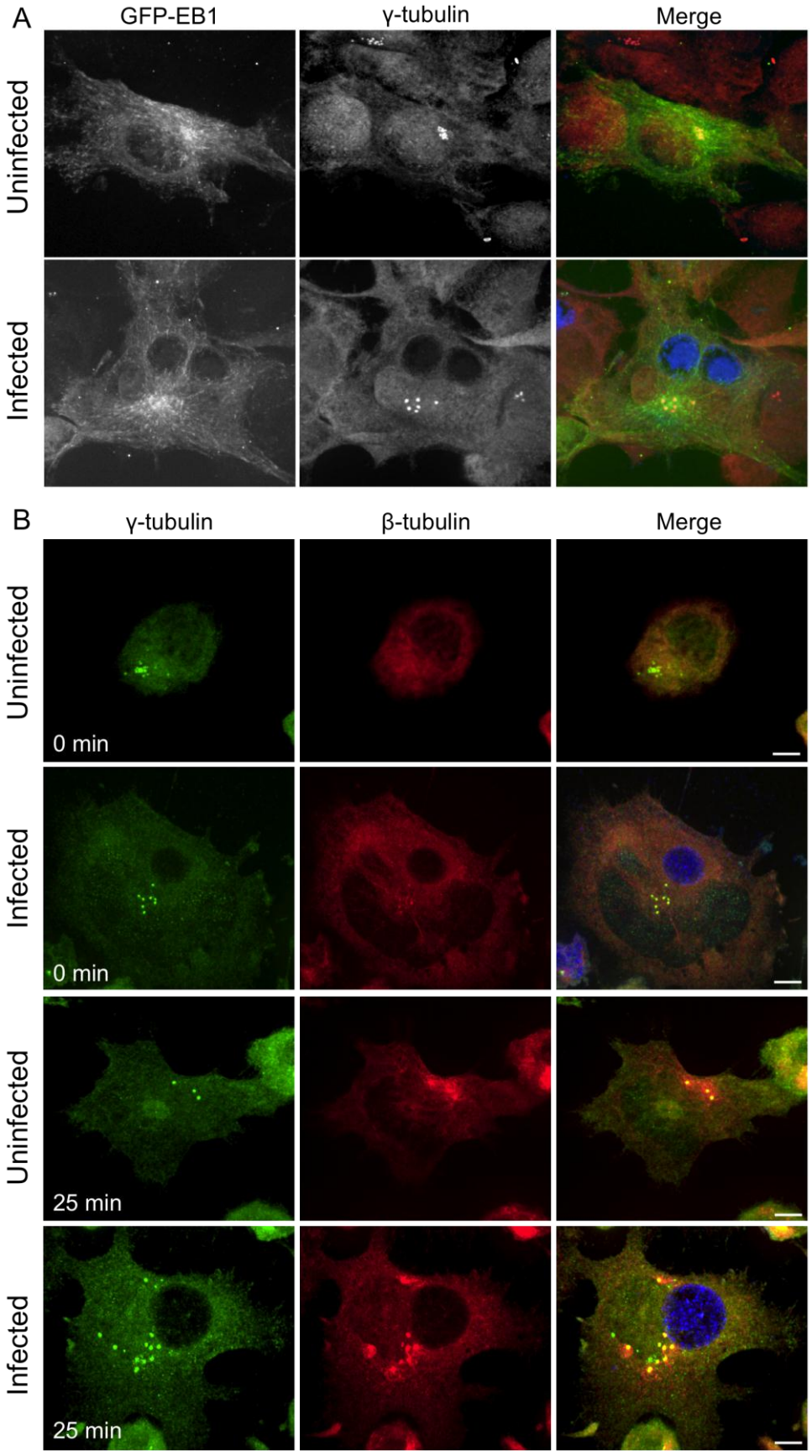
A
GFP-EB1
γ-tubulin
Merge
Uninfected
Infected
B
γ-tubulin
β-tubulin
Merge
Uninfected
0 min
Infected
0 min
Uninfected
25 min
Infected
25 min

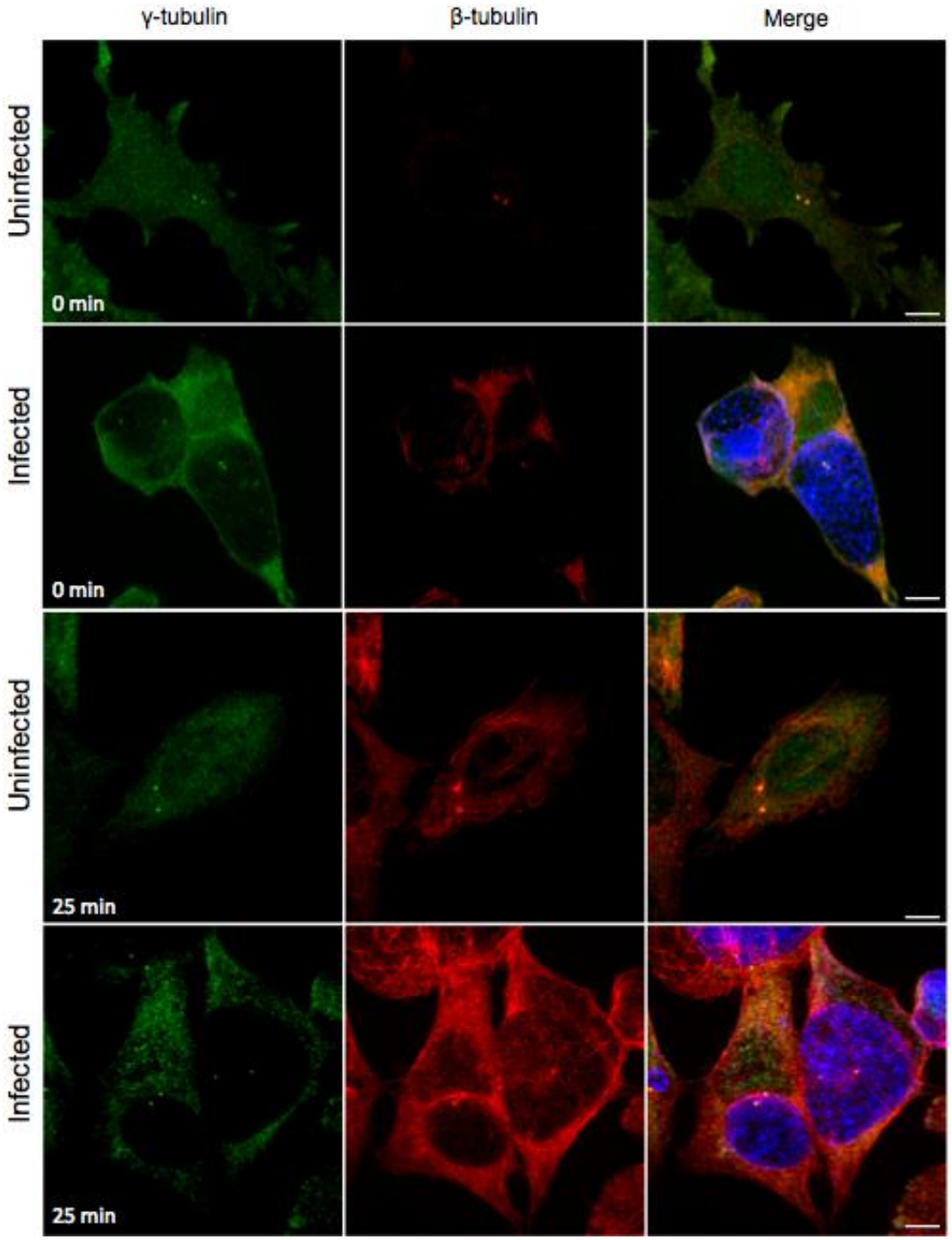


Figure 3-4. Chlamydial infection has no affect on centrosome ability to nucleate microtubules. HeLa cells were incubated with nocodazole and allowed to recover. The cells were fixed and stained at sequential time points during recovery for centrosomes (green), microtubules (red), and *Chlamydia* (blue) as necessary. The panels at time zero exhibit confocal images of cells at the time of washout. The panels at 25 minutes display cells that have been allowed to recover for 25 minutes after washout. Scale bars, 5μm

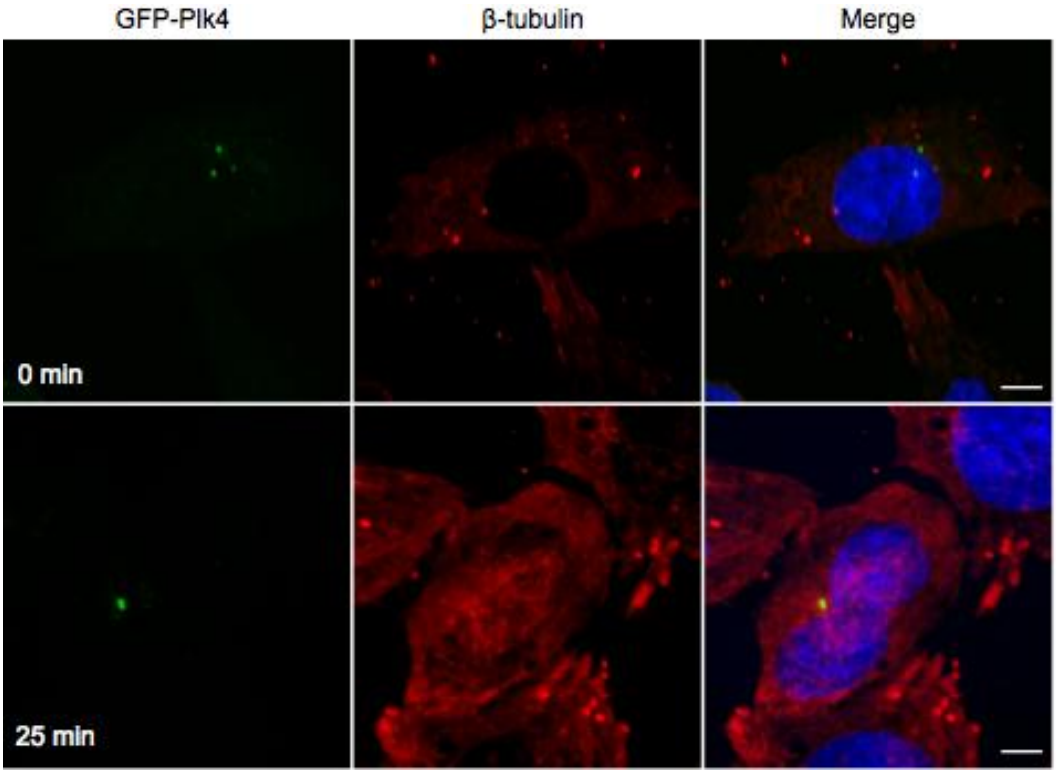


Figure 3-5. Plk4-induced extra centrosomes have no affect on centrosome ability to nucleate microtubules. HeLa cells were transfected with GFP-Plk4 incubated with nocodazole and allowed to recover. The cells were fixed and stained at sequential time points during recovery for centrosomes (green), and microtubules (red). The panels at time zero exhibit confocal images of cells at the time of washout. The panels at 25 minutes display cells that have been allowed to recover for 25 minutes after washout. Scale bars, 5μm.

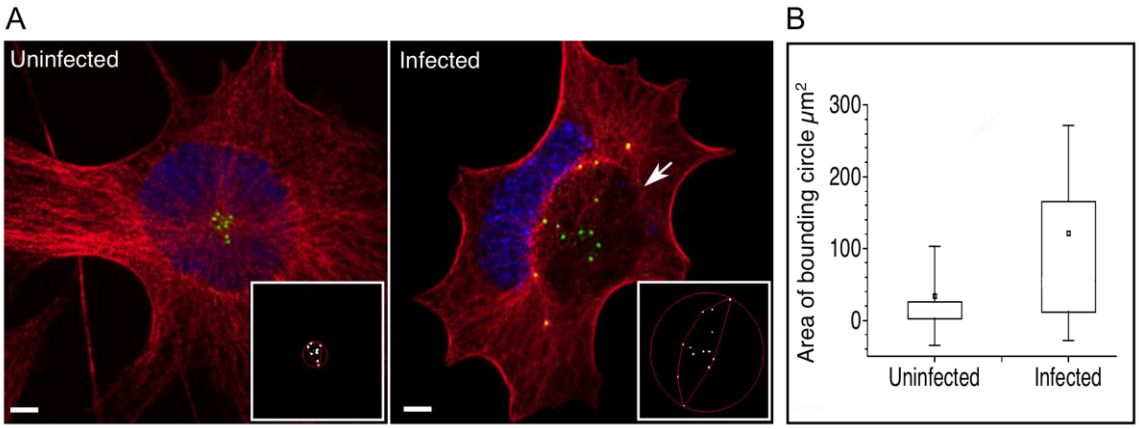


Figure 3-6. Chlamydial infection affects centrosome positioning in interphase cells. A) Both uninfected and infected neuroblastomas were stained for centrosomes (green), microtubules (red), and DNA (blue). The chlamydial inclusion is demarcated with an arrow. The area within the bounding circle translates to the geometric spread of the centrosomes (inset). B) The box and whisker plot demonstrates the uninfected population have centrosomes that are clustered within an average area of 34.4μm$^2$ (small box) ± 69.1 (standard deviation, whiskers), and the middle 50% of uninfected cells have centrosomes clustered within an area of 1.5 to 24μm$^2$ (large box). The infected cells contain centrosomes that are spread over a larger distance with a mean average area of 121.9μm$^2$ ± 149.8, with the middle 50% spread between 10 and 164.5μm$^2$, n < 76 for each population. Scale bars, 5μm.

Figure 3-7. Dynein localization and function is unaffected by chlamydial infection. A) ImageJ was used to measure the relative fluorescence intensity of uninfected and infected cells stained with anti-dynein IC (mAb 74.1). Figure A demonstrates how the images are processed. Scale bars, 5μm. B) The relative dynein percentages in the spindles of the infected and uninfected populations was measured, $n > 50$, and the experiment was repeated three times. The uninfected cells contain $18.4 \pm 1$ percent dynein in the spindles and the infected cells contain $32.7 \pm 2$ percent dynein, $^*p < 0.0001$ (Student's t-test). C) This was confirmed by western blot. D) Dynein trafficking function was determined by measuring the delivery of Alexa-transferrin (Tf) or Alexa-Cholera toxin B subunit (CtxB) to the peri-nuclear region of the cell in uninfected and infected cells. The fluorescence intensity of Tf and CtxB was determined at 0, 15, and 30 minutes post incubation with the endocytic markers. There was no significant difference in the delivery of Tf or CtxB in uninfected or infected cells. E) Furthermore, dyenin-dependent delivery of *Chlamydia* serovar L2 was not affected by previous infection of cells with serovar G.

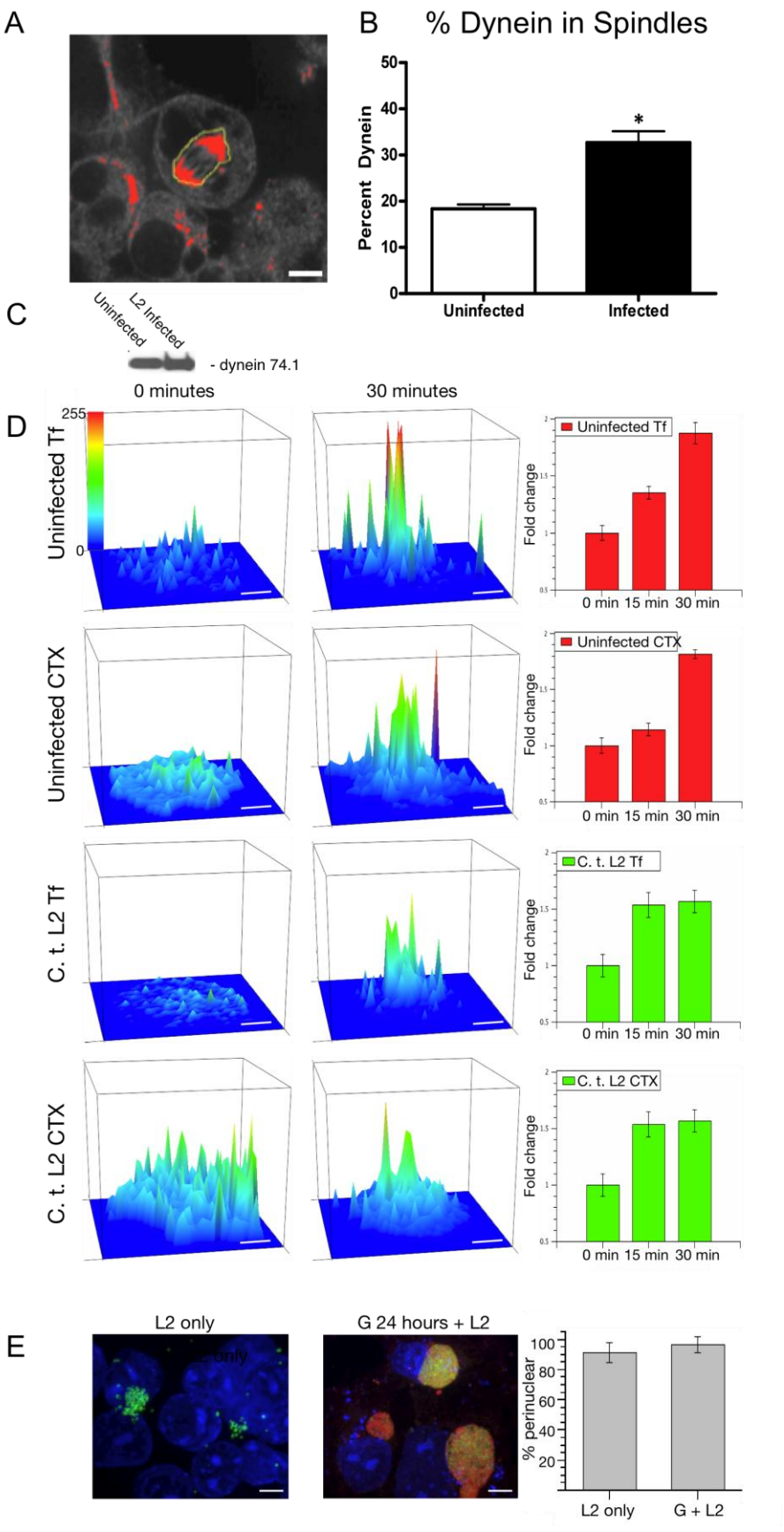
A
B % Dynein in Spindles
Percent Dynein
50
40
30
20
10
0
*
Uninfected
Infected
C
Uninfected
L2 Infected
- dynein 74.1
D
0 minutes
30 minutes
255
0
Uninfected Tf
Uninfected CTX
C. t. L2 Tf
C. t. L2 CTX
Fold change
0 min 15 min 30 min
E
L2 only
G 24 hours + L2
% perinuclear
100
80
60
40
20
L2 only
G + L2

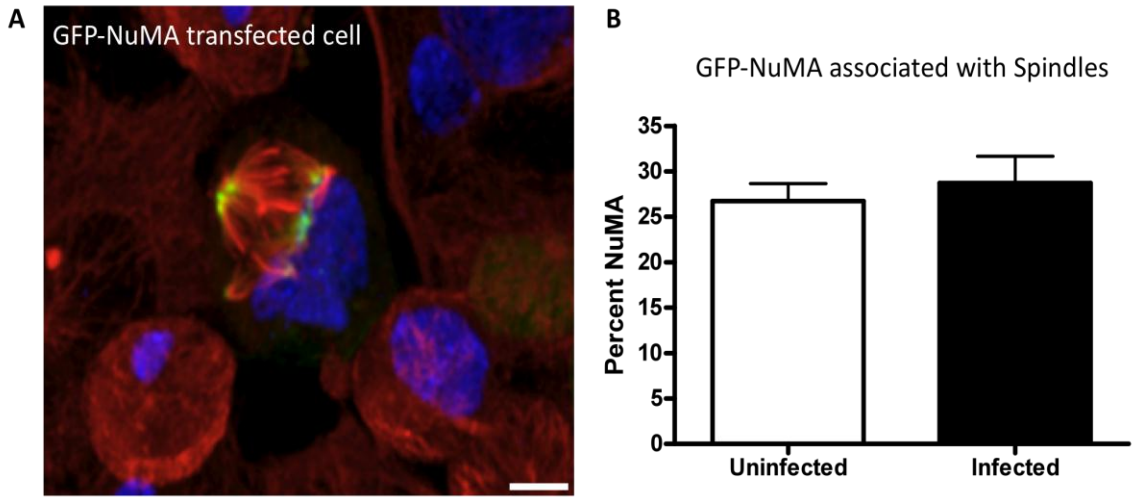


Figure 3-8. Chlamydial inhibition of centrosome clustering occurs independently of NuMA. A) Neuroblastomas were transfected with the construct GFP-NuMA. Mitotic, GFP-NuMA-positive cells were measured for NuMA association with the spindles using ImageJ. The spindles were stained with β-tubulin (red), and *Chlamydia* (blue). Scale bars, 5μm. B) There was no significant difference in the in the relative amount of NuMA associated with the spindles in uninfected or infected populations, 26.7 ± 2 and 28.7 ± 2 percent, respectively.

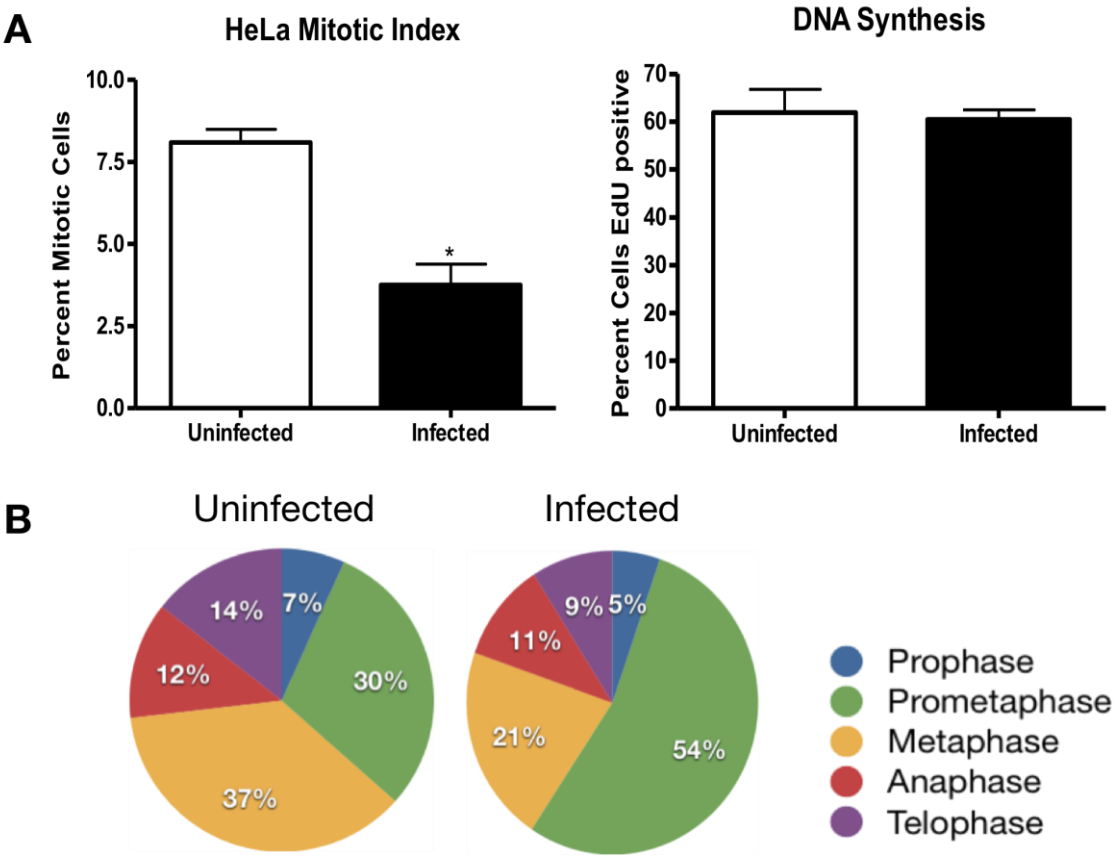


Figure 3-9. Examination of the cell cycle demonstrates *Chlamydia* overrides the SAC. A) The mitotic index of infected cells significantly decreases from 8.1 ± 0.4 to 3.8 ± 0.6 percent mitotic uninfected cells, $p = 0.0044$. The rates of DNA synthesis in HeLas measured by incorporation of EdU, remained the same in uninfected and infected cells (62 ± 4.8 vs 60.5 ± 5.2 percent cells positive for EdU). B) Analysis of uninfected and infected (32hrs) HeLa cells during the different stages of mitosis revealed that cells undergo a shift from metaphase (36.6 ± 1.3 percent cells in metaphase) to prometaphase (54.0 ± 3.2 percent cells in prometaphase) during infection, $p < 0.001$ (Student's t-test).

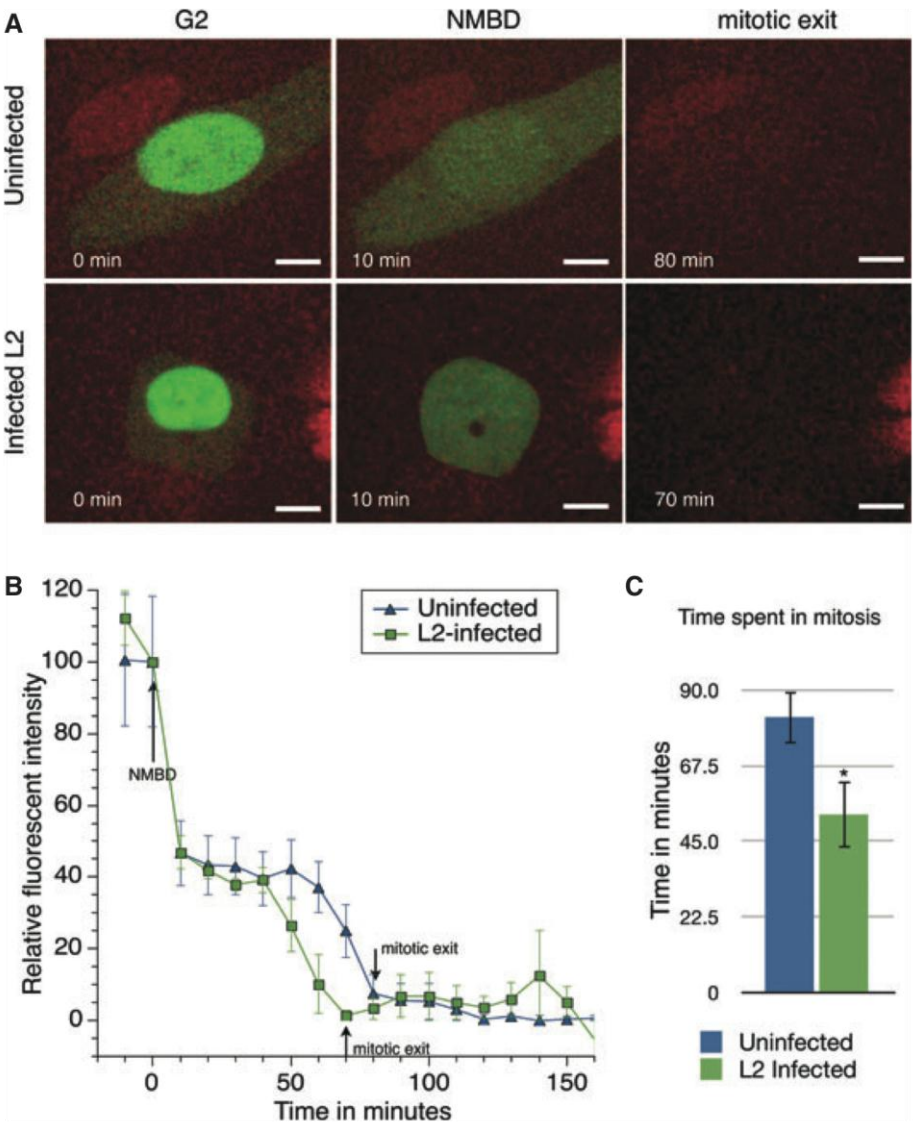


Figure 3-10. *Chlamydia* induces early mitotic exit as shown by FUCCI analysis. HeLa cells were transduced with FUCCI and imaged live by confocal microscopy. Time spent in mitosis was determined by assessing the time from nuclear membrane breakdown (NMBD) to complete degradation of GFP. A) Each panel contains a representative image from uninfected and infected cells in G2 (0 minutes), the start of mitosis (NMBD, 10 minutes), and mitotic exit (variable time). Scale bars, 5μm. B) The relative fluorescence intensity is normalized to time zero and the plot displays the decrease in fluorescence intensity from NMBD to mitotic exit (arrows). Each point represents the average normalized fluorescence intensity for 4 infected cells and 5 uninfected cells. C) The average time spent in mitosis is quantified in the graph. The time for uninfected cells is 53 ± 3 minutes, and 82 ± 8 minutes for infected cells, p = 0.018.

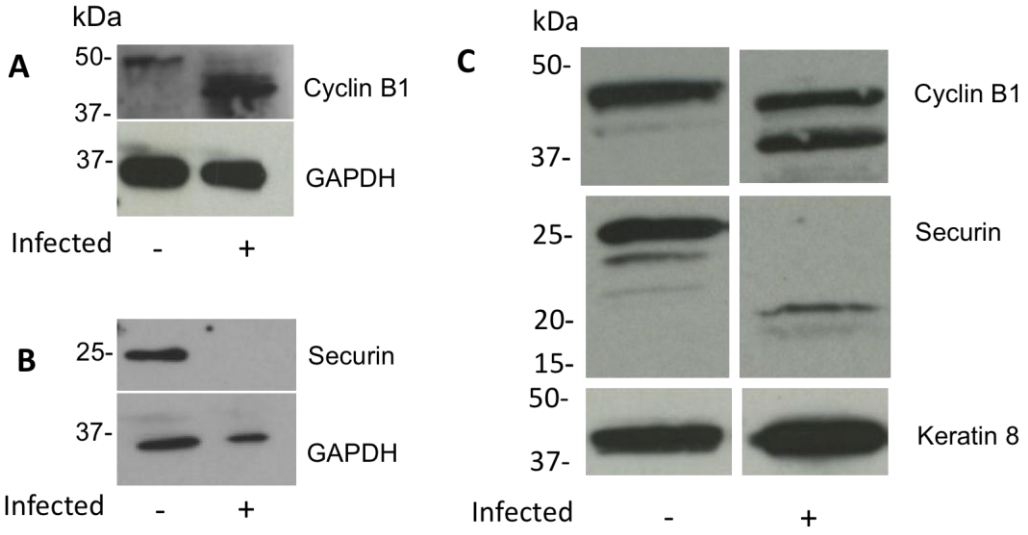


Figure 3-11. Chlamydial infection leads to the degradation of cyclin B1 and securin. Uninfected and infected lysates of HeLa cells were examined for the SAC proteins cyclin B1 and securin. A) Western blot analysis of uninfected and infected lysates for cyclin B1 displayed cleavage of cyclin B1. B) Securin was analyzed by IP followed by western blot analysis which also demonstrated degradation in infected lysates. C) A cell-free degradation assay was performed. Cyclin B1 and securin cleavage occurs in the presence of cytosolic chlamydial proteins.

# CHAPTER 4
# EVIDENCE OF CHLAMYDIAL INDUCED CELL DEFECTS *IN VIVO*

## ***Chlamydia* Affects Dividing Cells *In Vitro* and *In Vivo***

*Chlamydiae* are bacterial pathogens that infect epithelial cells and are responsible for a wide range of diseases in both animal and human hosts. *Chlamydia trachomatis*, a human pathogen, is comprised of over 15 distinctive serovars some of which are responsible for trachoma; the leading cause of preventable blindness, as well as the most commonly acquired sexually transmitted infection of bacterial origin. In women, untreated genital infections can result in devastating consequences such as pelvic inflammatory disease, ectopic pregnancy, and even infertility (Schachter, 1999; Belland et al., 2004). Every year, there are over 4 million new cases of Chlamydia in the United States (Miller et al., 2004) and an estimated 92 million cases worldwide (WHO, 2001). This study will also focus on *Chlamydia muridarum*, formerly the murine serovar of *C. trachomatis* referred to as mouse pneumonitis (MoPn). Despite the differences in tissue tropism *C. trachomatis* and *C. muridarum* share a very similar genome (Stephens et al., 1998; Read et al., 2000) Although *C. muridarum* causes no known disease in humans it is extensively used as a model in studying human reproductive tract disease, as infection of mice with *C. muridarum* closely resembles the pathology of genital infection with *C. trachomatis* (Patton et al., 1989; Cotter et al., 1995; Shah et al., 2005).

Infection with *Chlamydia trachomatis* has been epidemiologically linked to increased rates in cervical cancer in women who are co-infected with human papillomavirus (HPV) (Koskela et al., 2000; Anttila et al., 2001; Smith et al., 2002; Wallin et al., 2002; Matsumoto et al., 2003; Hinkula et al., 2004; Smith et al., 2004; Madeleine et al., 2007). Cervical cancer is the second most common cancer of women worldwide

(Woodman et al., 2007). Greater than 90% of cervical cancers are associated with high risk HPV types 16 and 18, but there is a considerable time gap between exposure to HPV and development of cervical cancer (Walboomers et al., 1999). This is attributed to the fact that HPV is a necessary but insufficient cause of cervical cancer, and many studies have been conducted to investigate other risk factors that are involved in progression of the disease, including smoking, exposure to hormones, and the host's immune system among others (zur Hausen, 1996; Madeleine et al., 2007).

We have previously shown that chlamydial infection stimulates aberrant centrosome amplification. Centrosome abnormalities result in spindle architecture defects during mitosis, and chlamydial induced defects during mitosis lead to chromosomal segregation errors, failure in cytokinesis, and aneuploidy (Grieshaber et al., 2006; Knowlton et al., 2011; Brown et al., 2012). These cellular defects are apparent in cancerous lesions of almost every origin (Pihan et al., 1998; Lingle et al., 2002; zur Hausen, 2002; Pihan et al., 2003; Nigg, 2006; Ganem et al., 2009). We hypothesize that the transformative phenotypes *Chlamydia* infection induces *in vitro* can contribute to transformative defects *in vivo.*

In this study we show host cell division is a major requirement for chlamydial induced cell defects to arise. We demonstrate chlamydial infection can transform 3T3 cells *in vitro* leading to anchorage independence and the formation of colonies in soft agar. We utilize a mouse model to demonstrate *Chlamydia muridarum* is able to infect actively replicating cells *in vivo*. We also determine infection with *Chlamydia* induces significant increases in cell proliferation within the cervix in mice that are transgenic for HPV oncoprotein E7 as well as their wild-type littermates. This infection corresponds

with progression to moderate cervical dysplasia in these mice. The development of cervical dysplasia is likely an important factor in defining a role for *Chlamydia* in cervical cancer development.

## Results

### The Chlamydial Induced Cytopathic Effects of Centrosome Amplification, Multipolar Spindles, and Multinucleation are Dependent on Cellular Replication and Not Dependent on Coexpression of Any Particular Oncogenes

We have previously described that chlamydial infection induces multipolar spindles, centrosome amplification, and multinucleation in HeLa cells. HeLa cells are a cervical cancer cell line that express components of the HPV18 genome including the E6 and E7 oncoproteins (Schwarz et al., 1985). We and others have demonstrated that the induction of multipolar spindles, centrosome amplification, and multinucleation all require progression through the cell cycle (Greene and Zhong, 2003; Johnson et al., 2009; Knowlton et al., 2011). To determine if the oncogenes expressed in HeLa cells were required for any of these phenotypes we measured the rates of centrosome amplification, multipolar spindle formation, and multinucleation in a variety of cells that replicate in culture (Figure 4-1). We tested End1/E6E7, COS-7, and 3T3 cells. End1 (ATCC CRL-2615) cells are an endocervical cell line established from normal epithelial tissue and immortalized by transduction with the retroviral vector LXSN-16E6E7 (Fichorova et al., 1997). These cells express the E6 and E7 oncogenes from HPV-16. COS-7 cells are an African green monkey kidney fibroblast-like cell line derived by transformation with an origin defective mutant of SV40 which codes for wild-type T antigen (Gluzman, 1981). The 3T3 cell line was established from disaggregated Swiss mouse embryos and spontaneously developed immortality but retain anchorage dependence (Todaro and Green, 1963).

We infected End1, COS-7, and 3T3 cells for 36 hours with *C. trachomatis*, serovar L2. We chose this time point because it corresponds with centrosome and spindle abnormalities as we have previously described. Compared with their uninfected counterparts End1 cells had elevated numbers of centrosomes, from 2.5 ± 0.1 to 3.5 ± 0.1 centrosomes/cell, respectively. These cells also displayed a significant increase in multipolar spindle formation, from 21.2 ± 4.6 percent in uninfected cells to 73.7 ± 2.0 percent. Upon infection End1 cells also demonstrated a significant increase in the percentage of multinucleated cells from 6.7 ± 0.8 to 36.6 ± 3.3 percent (Figure 4-1A). We also investigated COS-7 cells, and upon infection had increased numbers of centrosomes, from 2.1 ± 0.03 centrosomes/cell to 2.8 ± 0.2, respectively. There was also a significant increase in the formation of multipolar spindles after chlamydial infection from 15.5 ± 0.8 percent multipolar to 30.0 ± 2.9 percent. Multinucleated cells accumulated significantly from 13.9 ± 1.9 percent to 37.1 ± 0.8 percent multinucleated (Figure 4-1B). The 3T3 fibroblasts displayed a similar trend, with a significant increase in centrosome number from 2.2 ± 0.1 to 3.2 ± 0.1 centrosomes/cell. The formation of multipolar spindles increased significantly from 5.5 ± 0.9 percent multipolar to 41.2 ± 3.5 percent. The presence of multinucleated 3T3s increased moderately from 2.9 ± 0.01 percent to 4.8 ± 0.1 percent multinucleated (Figure 4-1C). Although the 3T3 cells had only a modest but significant increase in multinucleated cells infection with *Chlamydia* was still able to induce centrosome abnormalities and spindle assembly difficulties. In all cases after infection the cells contained amplified centrosomes, increased rates of multipolar spindles and an accumulation of multinucleated cells. These results support

the hypothesis that the only cellular cofactors required for these phenotypic effects is cellular replication.

**Infection of NIH3T3 Cells Induces Anchorage Independence**

To determine if these potentially transforming phenotypes induced by chlamydial infection could lead to cellular transformation we infected 3T3 cells with *C. trachomatis* L2 at a MOI of 10 to reach a high probability that every cell was infected. These cells were cured of the infection with rifampicin for four days and allowed to recover for an additional three days. The cured 3T3 cells were then plated in soft agar and allowed to grow for 28 days (Figure 4-2B). *In vitro* cellular transformation detection assays are commonly used to measure the morphological changes in cellular phenotypes induced by carcinogens and other insults (DiPaolo et al., 1969; Lasne et al., 1974; Yoheved et al., 2004). Transformation associated with phenotypic changes, such as 3T3 anchorage-independent growth, can be easily assayed by quantifying colony formation in soft agar (Shin et al., 1975).

When infected and cured 3T3s were plated in soft agar we saw a significant increase in colony formation compared to mock-infected and cured 3T3s; the mock-infected cells had an average of $1.7x10^{-4} \pm 3.1x10^{-5}$ colonies/well, and the cured 3T3s had a dramatic increase in colony formation with an average of $1.5x10^{-3} \pm 2.6x10^{-4}$ colonies/well (Figure 4-2A). As a control for transformation we exposed 3T3 cells to ultraviolet (UV) light for 1, 3, and 5 minutes. We saw a significant increase in colony formation at 1 and 3 minutes compared to mock-infected colonies, $9.9x10^{-4} \pm 1.5x10^{-4}$ colonies/well and $1.8x10^{-3} \pm 2.9x10^{-4}$, respectively. At 5 minutes of UV exposure there was a decrease in the number of colonies/well compared to 1 and 3 minutes, at $1.4x10^{-3} \pm 1.6x10^{-4}$, and we attribute this to cell death due to excessive DNA damage from UV

exposure. To verify that colony formation from infected and cured cells was a *Chlamydia*-specific effect and not the result of intracellular infection or of secondary effects from a large bolus of material like the inclusion, we also infected cells with the obligate intracellular bacterium *Coxiella burnetii*. *C. burnetii* lives within a parasitophorous vacuole (PV) inside the host cell, and the volume of the *Coxiella* PV can occupy a large portion of the cytoplasm much like the chlamydial inclusion (Howe and Heinzen, 2006). When we infected and cured 3T3 cells of *C. burnetii* infection there was no increase in colony formation compared to mock-infected controls at $3.3x10^{-5}$ ± $2.3x10^{-5}$ colonies/well. The resulting colony formation indicates that *Chlamydia trachomatis* has the ability to induce transformation of 3T3 cells *in vitro*, supporting our hypothesis that cellular defects that arise due to chlamydial infection have potentially detrimental effects.

**Reproductive Tract Infection of Mice Demonstrates *Chlamydia* Infects Replicating Cell Populations**

*Chlamydia trachomatis* causes sexually transmitted disease infecting the epithelial cells of the vagina, cervix, uterus, and Fallopian tubes. This population of cells is terminally differentiated but does undergo cyclical cell turnover and replacement; consequently there is a subset of cells undergoing cellular replication (Leppert, 2012). We used the mouse model of chlamydial infection to ascertain *Chlamydia's* ability to infect those replicating cell populations. We infected 8 week old wild-type FVB/N mice with *Chlamydia muridarum* for 7 days, and injected them with EdU (5-ethynyl-2'-deoxyuridine), a thymidine analog, for three consecutive days prior to sacrifice. The EdU allowed us to visualize any cells that had undergone S-phase, as the thymidine analog would have been taken up by any newly synthesized DNA (Salic and Mitchison,

2008). We examined EdU-treated tissue sections co-stained for *Chlamydia* and DNA, and we observed a subset of infected actively replicating cells within the cervical epithelium (Figure 4-3A).

**Infection Stimulates Cellular Replication During Infection**

Chlamydial infection begins in the vaginal epithelium, ascending toward the cervix and the upper genital tract. The epithelium lining the vagina and the outer cervix is composed of squamous epithelium. Where the outer cervix meets the inner cervix the squamous epithelium is replaced by glandular columnar epithelium, and the columnar epithelium lines the inner cervix and the rest of the upper genital tract. The junction on the cervix where squamous epithelium transitions to columnar epithelium is known as the transformation zone. Because of the high degree of metaplasia, or the process of one type of epithelium transitioning into another, most cervical cancers originate in the transformation zone (Autier et al., 1996; Elson et al., 2000).

We wanted to investigate the native replication rate of the cells in the transformation zone, and whether a 7 day chlamydial infection could change the level of replicating cells in this region. We compared the replication rates in these cells with a HPV-16 E7 gene knock-in mouse. These mice were created as a model for HPV-induced cervical cancer in an effort to elucidate the E7 oncogene specific contributions to cancer progression. The expression of the E7 oncogene is driven under the human keratin 14 (K14) promoter, its expression directed to the stratified epithelium, therefore the mouse is designated as K14-HPV-E7 (Herber et al., 1996). We chose to examine the E7 knock-in mouse because expression of the transgene would ensure these mice to have increased cellular replication rates over the wild-type animals. We were also interested in distinguishing whether chlamydial infection could exacerbate this increased

replication. These animals were treated with exogenous estrogen, as it has been shown to be an essential cofactor in the onset and development of cervical cancer in this mouse model (Brake and Lambert, 2005). We elected to treat both the transgenic and wild-type groups with estrogen to provide each animal matched capacity to develop cervical dysplasia, and to identify any chlamydial specific effects during this process.

To determine the proliferation rates of the cervical epithelium in these animals we calculated the percentage of EdU positive cells present over multiple fields of view within the transformation zone (Figure 4-3B). The wild-type, mock-infected animals had a native cell proliferation rate of 3.0 ± 0.5 percent and upon infection this rate increased significantly to 21.7 ± 5.9 percent. The K14-HPV-E7 mice had a native replication rate of 5.7 ± 1.0 percent, and the infected K14-HPV-E7 animals had a considerably higher proliferation rate of 19.7 ± 2.6 percent. We believe the increase in cell proliferation rates due to chlamydial infection can be attributed to remodeling of the epithelial lining after the insult of infection. This remodeling however, gives *Chlamydia* overwhelming access to actively replicating cells, resulting in the opportunity to induce transformative defects within the host cell. The bacterial load for each infected animal was calculated based on recovered inclusion forming units (IFUs) (Morrison et al., 2011) enumerated in Table 4-1.

**Chlamydial Infection Induces Cervical Dysplasia in Mice**

We next wanted to investigate the effects of chlamydial infection on cervical histopathology. Cervical cancer arises from noninvasive premalignant lesions known as cervical intraepithelial neoplasias (CINs). In women these lesions are graded histologically based on the presence of atypical epithelial cells on the outer cervix: CIN I correlates with mild dysplasia, CIN II with moderate dysplasia, and CIN III corresponds

to both severe dysplasia and carcinoma *in situ* (Steenbergen et al., 2005). A board certified pathologist blinded to experimental condition surveyed the groups of mock-infected and infected K14-HPV-E7 mice and their wild-type littermates used above, and assigned a pathological score to two different sections from each animal. The rubric is detailed in the methods section. These scores were established by a grading system developed specifically for HPV transgenic mice to determine the degree of dysplasia in the mouse cervix (Riley et al., 2003). This classification system is based on the human model for carcinogenic progression mentioned above. We compared these scores between uninfected and infected animals to determine if chlamydial infection induced cervical dysplasia (Figure 4-4A). The wild-type, mock-infected group retained normal cervical epithelium after treatment, receiving an average score of 1.3 ± 0.3. The wild-type infected group however, progressed to moderate cervical intraepithelial neoplasia with a CIN score of II receiving an average score of 3.3 ± 0.3. The K14-HPV-E7 mice followed the same trend with the uninfected group receiving a score of 1.8 ± 0.5 indicating the normal epithelium was preserved after treatment, while the infected group received a score of 3.5 ± 0.3 revealing these animals also progressed to CIN II. The normal tissue from both wild-type and transgenic animals contains cells with normal nuclear to cytoplasm ratio and mitotic figures present only in basal layers (Figure 4-4B). CIN II lesions contain cells with increased nuclear size, some anaplastic cells, and dysplastic cells distributed frequently throughout the squamous epithelium. The lesions are also characterized by epithelial projections thrown into the underlying cervical stroma (Figure 4-4C). The presence of moderate cervical dysplasia in the infected animals suggests that, at least initially, *Chlamydia* is able to provide a convenient

environment for cervical dysplasia progression. The CIN II score the infected K14-HPV-E7 animals received also indicates that chlamydial infection may play a role in exacerbation of cellular defects contributed by HPV oncogene expression.

**Indication of Chlamydial Induced Cellular Defects *in Vivo***

Finally, we wanted to determine if any of the phenotypic evidence of pre-cancerous and cancerous lesions we identified in cell culture existed *in vivo*. Because we showed *Chlamydia* was able to infect actively replicating cells and there was such an abundance of cell proliferation upon infection we chose to infect the animals on day 0 and reinfect on day 3 of the one week infection. This increased the probability of infection within replicating cells. We then examined the vaginal and cervical tissue for centrosome defects, spindle multipolarity, and presence of multinucleated cells in both K14-HPV-E7 mice and wild-type. Contrary to the 5μm thick tissue sections we evaluated above for the cell proliferation experiments and histopathology, these experiments surveyed tissue sections 10μm thick, which encompasses the depth of a layer of cells in its entirety. We could then be assured we were examining an entire cell in three-dimensional space.

We found evidence of centrosomes associated the chlamydial inclusion, rather than the juxtanuclear position they normally occupy (Figure 4-5A). We have previously reported that chlamydial infection leads to the physical separation of centrosomes, resulting in difficulty positioning them appropriately for cell division (Knowlton et al., 2011). We also observed infected cells with more than one nucleus (Figure 4-5B). Multinucleation is a phenotype associated with chromosomal instability, low and high grade cervical dysplasia, and we have shown chlamydial infection can induce multinucleation in cultured cells (Duensing et al., 2001; Riley et al., 2003; Brown et al.,

2012). To establish nuclei were, in fact, inside a single cell we co-stained our sections with an antibody for the transmembrane protein E-cadherin. E-cadherin is expressed specifically in epithelial tissues and the antibody staining allowed us to visualize the membrane for individual cells. Further inspection of our tissue sections also resulted in the discovery of a micronucleus in an infected cell (Figure 4-5C). Micronuclei are small cytoplasmic bodies containing chromatin that are morphologically similar to nuclei, but are not included in daughter nuclei after cell division. They are the result of a number of factors including acentric chromosome fragments (chromosomes lacking a centromere) due to ionizing radiation or excision repair of damaged bases. Micronuclei have also been shown to be the product of mis-segregation of whole chromosomes during anaphase either due to a disruption in mitotic spindle assembly, defects in the spindle assembly checkpoint (SAC), or abnormal centrosome amplification (Kirsch-Volders et al., 1997; Gisselsson, 2008; Zyss and Gergely, 2009; Fenech et al., 2011). Previous work to come out of our lab has demonstrated *Chlamydia* to be responsible for inducing spindle architecture defects, delaying the SAC, and stimulating centrosome amplification (Knowlton et al., 2011; Brown et al., 2012). We have also shown HeLa cells cured of an infection have increased rates of micronuclei formation (Grieshaber et al., 2006).

We did not find any infected cells undergoing mitosis in our tissue sections. We believe this is because mitosis is a comparatively quick process, and unlike cells in culture where *Chlamydia* infects almost 100% of the cells the level of infection is a great deal lower in animal tissue. Thus infected cells undergoing mitosis is a much rarer event in our tissue sections. Multinucleation, centrosome positioning defects and the formation

of micronuclei are phenotypes that accumulate and are therefore more readily observed in the infected tissues. However, the discovery of multinucleated cells and micronuclei leaves little doubt that chlamydial infection induces some level of chromosomal instability.

## Discussion

The epithelial lining of the genital tract is composed of terminally differentiated cells that undergo cyclical tissue remodeling leading to monthly cell turnover (Leppert, 2012). Because the epithelial cells are cyclically replaced by stem cells residing below the epithelial cell layer *Chlamydia* has little access to dividing cells. In this study we show that in cell culture a dividing cell population must be present to induce detrimental cellular defects such as abnormal proliferation of centrosomes, formation of multipolar spindles, and the presence of multinucleated cells; the coexpression of other oncoproteins appears not to be necessary. We believe the chlamydial induced defects to be responsible for the induction of anchorage independence in the 3T3 soft agar assay, as infection with *Coxiella burnetti* resulted in no colony formation. We understand there are differences in biology between murine and human cells, but with the support of cell defects present in human (HeLa) and primate (COS-7) cells, as well as 3T3s *in vitro*, we are confident in *Chlamydia's* ability to transform 3T3 cells in soft agar.

Due to a paucity of information regarding *Chlamydia's* affect on replicating cells *in vivo* we were curious to find out whether chlamydial infection could induce the same phenotypic defects *in vivo* as we have reported *in vitro* (Grieshaber et al., 2006; Knowlton et al., 2011; Brown et al., 2012). We were able to show for the first time that not only can *Chlamydia* infect actively replicating cells within the cervix of mice, but infection results in a considerable increase in cell proliferation in these animals. We

believe the induction of cell proliferation is significant because unchecked proliferation is the origin for cancer formation. The increased levels of cell replication upon infection create an environment predisposed for chlamydial induced centrosome aberrations, multipolar mitoses, and genetic instability. The increased replication rates in K14-HPV-E7 infected animals compared to their uninfected counterparts indicate *Chlamydia* may, in fact, exacerbate HPV-induced cell proliferation contributing to increased cellular defects, and perhaps contribute to the increased rates in cervical cancer that have been reported in women co-infected with HPV.

The development of moderate cervical intraepithelial neoplasia II in the infected mice was a surprising finding. We expected the K14-HPV-E7 mice to have some level of dysplasia due to the expression of the oncogene, as well as the wild-type mice to experience some mild cell changes as a result of infection, but we did not expect both wild-type and transgenic mice to develop CIN II. In future studies we will be interested to find out if this dysplasia persists or perhaps develops into carcinoma *in situ* over a 6 to 9 month period. We believe the cell proliferation induced by infection is a major contributing factor to cervical dysplasia, followed by chlamydial induced centrosome and mitotic spindle defects contributing to genetic instability. Furthermore, *in vivo* evidence of centrosome localization defects and genomic instability, which are present in precancerous and cancerous lesions of many origins, lends itself to the hypothesis that chlamydial infection may prime the cervix for progression to neoplasia or exacerbate neoplastic lesions already present.

Figure 4-1. *Chlamydia* induces centrosome and spindle defects in replicating cells. A) Uninfected and infected End1/E6E7 cervical carcinoma cells were stained for centrosomes (green, top and bottom panel), and mitotic spindles (green, middle panel), *Chlamydia* (red, infected panel) and DNA (blue). Uninfected cell populations have an average of 2.5 ± 0.1 centrosomes/cell, while the infected cell population centrosome distribution (arrow) significantly increased to an average of 3.5 ± 0.1 centrosomes/cell, $p<0.0001$, $N>150$. The number of cells with multipolar spindles (arrow) were counted for each population with the uninfected cells having 21.2 ± 4.6 percent multipolar spindles while the infected population significantly increased multipolar spindles to an average of 73.7 ± 2.0 percent, $p=0.0005$, $N>150$. The presence of multinucleated cells (stars) significantly increased with infection from 6.7 ± 0.8 to 36.6 ± 3.3 percent, $p=0.0009$, $N>200$. B) COS-7 cells were treated as above. Uninfected cells had an average of 2.1 ± 0.03 centrosomes/cell, infection resulted in an average of 2.8 ± 0.2 centrosomes/cell, $p=0.0200$, $N>300$. Uninfected COS-7s had an average of 15.5 ± 0.8 percent multipolar spindle formation, while the infected cells significantly increased to 30.0 ± 2.9 percent multipolar spindles, $p=0.0093$, $N>150$. When evaluated for the presence of multinucleated cells, uninfected populations had an average of 13.9 ± 1.9 percent multinucleated cells, and infected populations significantly increased to an average of 37.1 ± 0.8 multinucleated cells, $p=0.0003$, $N>200$. C) Uninfected and infected 3T3 fibroblasts were evaluated as the other cell lines above. Uninfected 3T3 cells had an average of 2.2 ± 0.1 centrosomes/cell, while infected cells increased significantly to 3.2 ± 0.1 centrosomes/cell, $p=0.0014$, $N>300$. Uninfected and infected populations of 3T3s were compared for multipolar spindle formation, uninfected cells had an average of 15.5 ± 0.9 percent multipolar spindles, while infected populations increased significantly to 41.2 ± 3.5 multipolar, $p=0.0021$, $N>150$. Uninfected 3T3s were 2.9 ± 0.01 percent multinucleated, and upon infection became 4.8 ± 0.1 percent multinucleated, a significant increase, $p<0.0001$, $N>200$. Scale bars, 5μm.

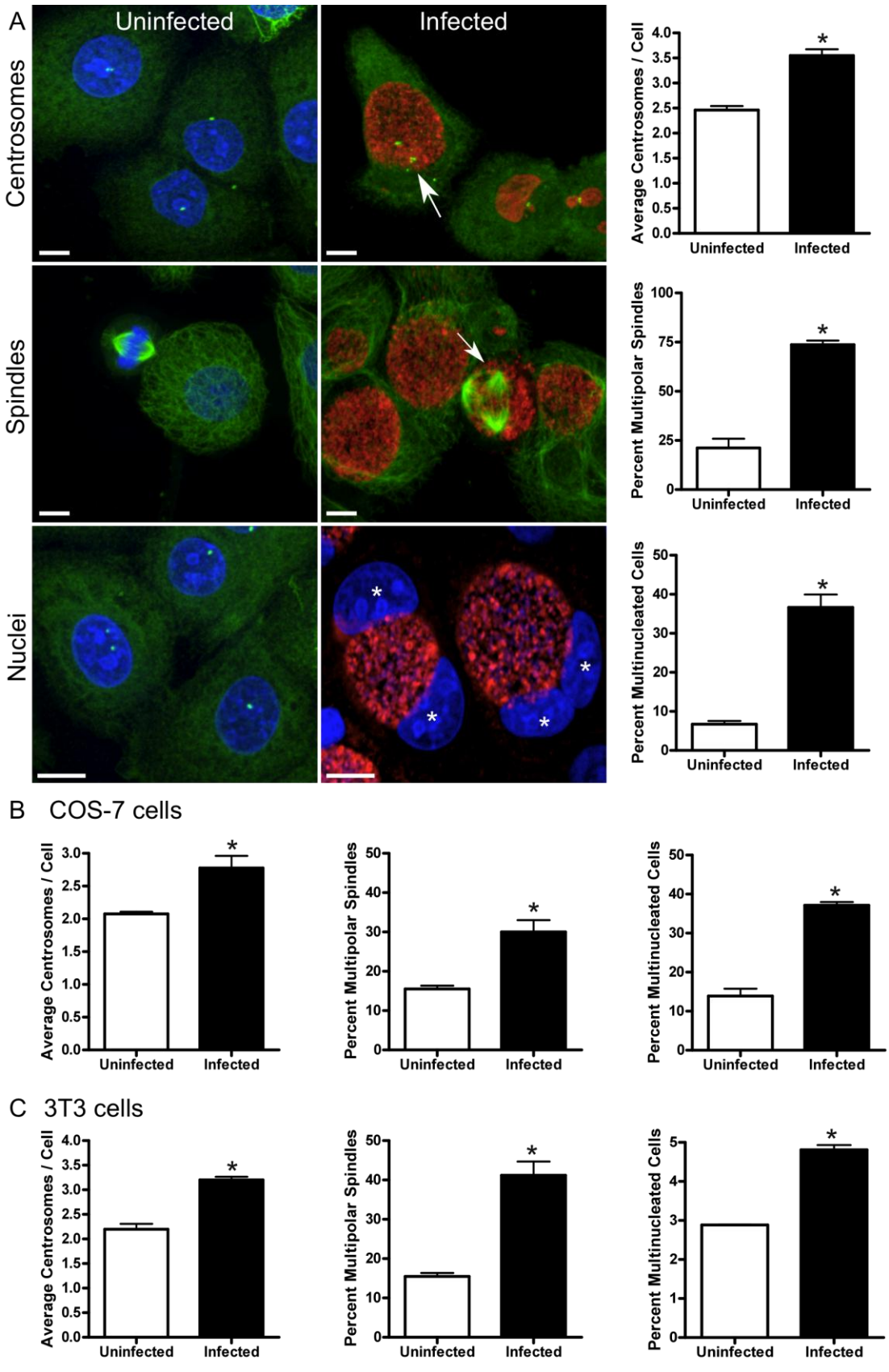
A
Uninfected
Infected
Centrosomes
Spindles
Nuclei
Average Centrosomes / Cell
Percent Multipolar Spindles
Percent Multinucleated Cells
Uninfected
Infected
B COS-7 cells
C 3T3 cells

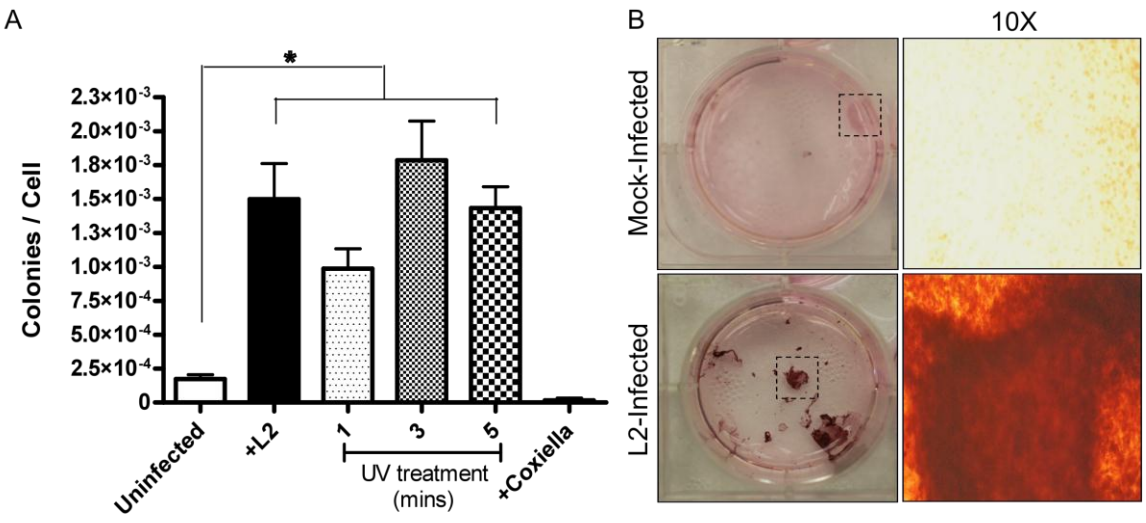


Figure 4-2. Chlamydial infection induces anchorage independence in 3T3 fibroblasts. Mock-infected and infected 3T3s were cured of chlamydial infection and incubated for 4 weeks in soft agar. The cells were stained, and the colonies were enumerated and normalized to the 2500 cells initially plated. A) The uninfected cells had an average of $1.7x10^{-4} \pm 3.1x10^{-5}$ colonies/well, the infected cells an average of $1.5x10^{-3} \pm 2.6x10^{-4}$ colonies/well. Cells treated with UV light for 1 minute had an average of $9.9x10^{-4} \pm 1.5x10^{-4}$ colonies/well, while cells treated for 3 and 5 minutes had an average of $1.8x10^{-3} \pm 2.9x10^{-4}$ and $1.4x10^{-3} \pm 1.6x10^{-4}$ colonies/well, respectively. 3T3 cells cured of an infection with the intracellular bacterial pathogen *Coxiella burnetii* had an average of $3.3x10^{-5} \pm 2.3x10^{-5}$ colonies/well. N>72 wells, $p<0.0001$. B) The images in the panels are examples of stained colonies from mock-infected and L2-infected cells after a 4 week incubation. The first column is a single well of a 6-well plate. The second column is a 10X magnification of the indicated area (dashed box).

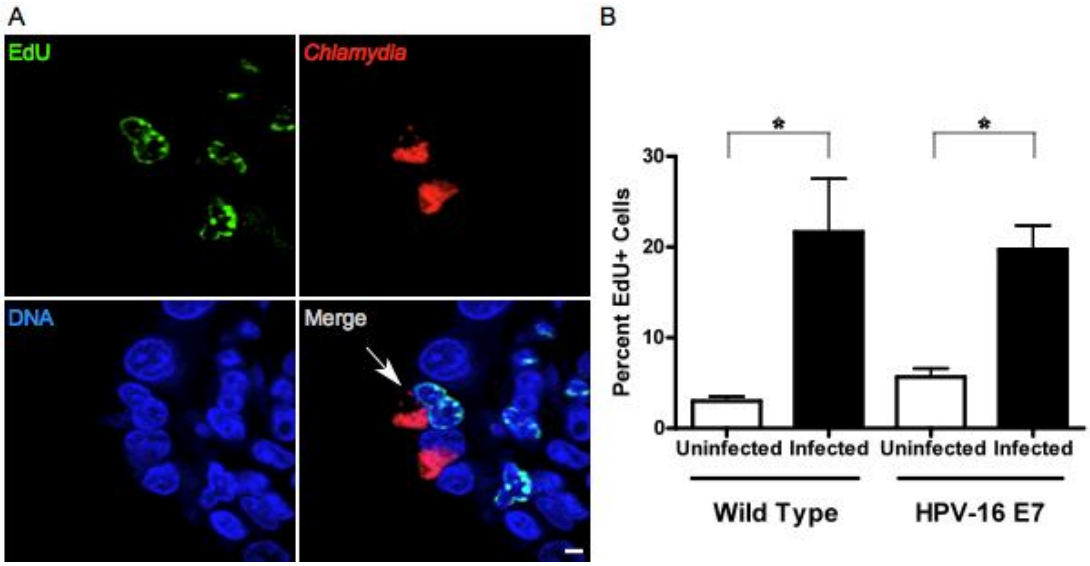


Figure 4-3. *Chlamydia* infects actively replicating cells *in vivo*, and induces cell proliferation. A) A female FVB wild-type mouse infected with *Chlamydia muridarum* for 7 days was treated with EdU (green) prior to sacrifice to detect cell proliferation, and formalin-fixed, paraffin-embedded sections (4μm thick) were stained for *Chlamydia* (red) and DNA (blue). The sections were imaged by confocal microscopy. A chlamydial inclusion can be seen associated with an actively replicating EdU positive cell (arrow) within the cervical epithelium. B) Female K14-HPV-E7 mice and their wild-type littermates were mock-infected and infected with *Chlamydia muridarum* for 7 days. The mice were treated with EdU, and the EdU positive cells per total cells present in multiple fields of view were counted to determine the rate of cell proliferation. Wild-type uninfected mice, N=4, had an average of 3.0 ± 0.5 percent cell proliferation, while the infected WT mice, N=3, experienced a significant increase of cell proliferation at an average of 21.7 ± 5.9 percent, p=0.003. The uninfected E7 mice had an average of 5.7 ± 1.0 percent cell proliferation, and the infected E7 mice had a significantly higher average of 19.7 ± 2.6 percent, p=0.0002, N=4 mice/group. Scale bars, 5μm.

Figure 4-4. Presence of *Chlamydia muridarum* induces CIN. Infected and mock-infected groups of 3-4 K14-HPV-E7 mice and their wild-type littermates were sacrificed 7 days post-infection. H&E sections were evaluated by a pathologist and each animal was given a score based on progression of cervical dysplasia; the scores were averaged for each animal. A) The wild-type, mock-infected group received an average score of 1.3 ± 0.3, N=4, indicating these animals retained normal cervical epithelium after treatment. The wild-type infected group received an average score of 3.3 ± 0.3, N=3 representing a progression to CIN II, p=0.0037. The K14-HPV-E7 mice followed a similar pattern with the uninfected group receiving a score of 1.8 ± 0.5 indicating most of the animals had normal tissue, while the infected group received a score of 3.5 ± 0.3 indicating these animals also progressed to CIN II, p=0.0203, N=4. B) Uninfected tissue from a wild-type and K14-HPV-E7 mouse. C) The CIN II lesions seen in the infected mice correspond with epithelial projections into the stroma and contain cells that have increased nuclear:cytoplasm ratio (arrows). Scale bars, 50μm.

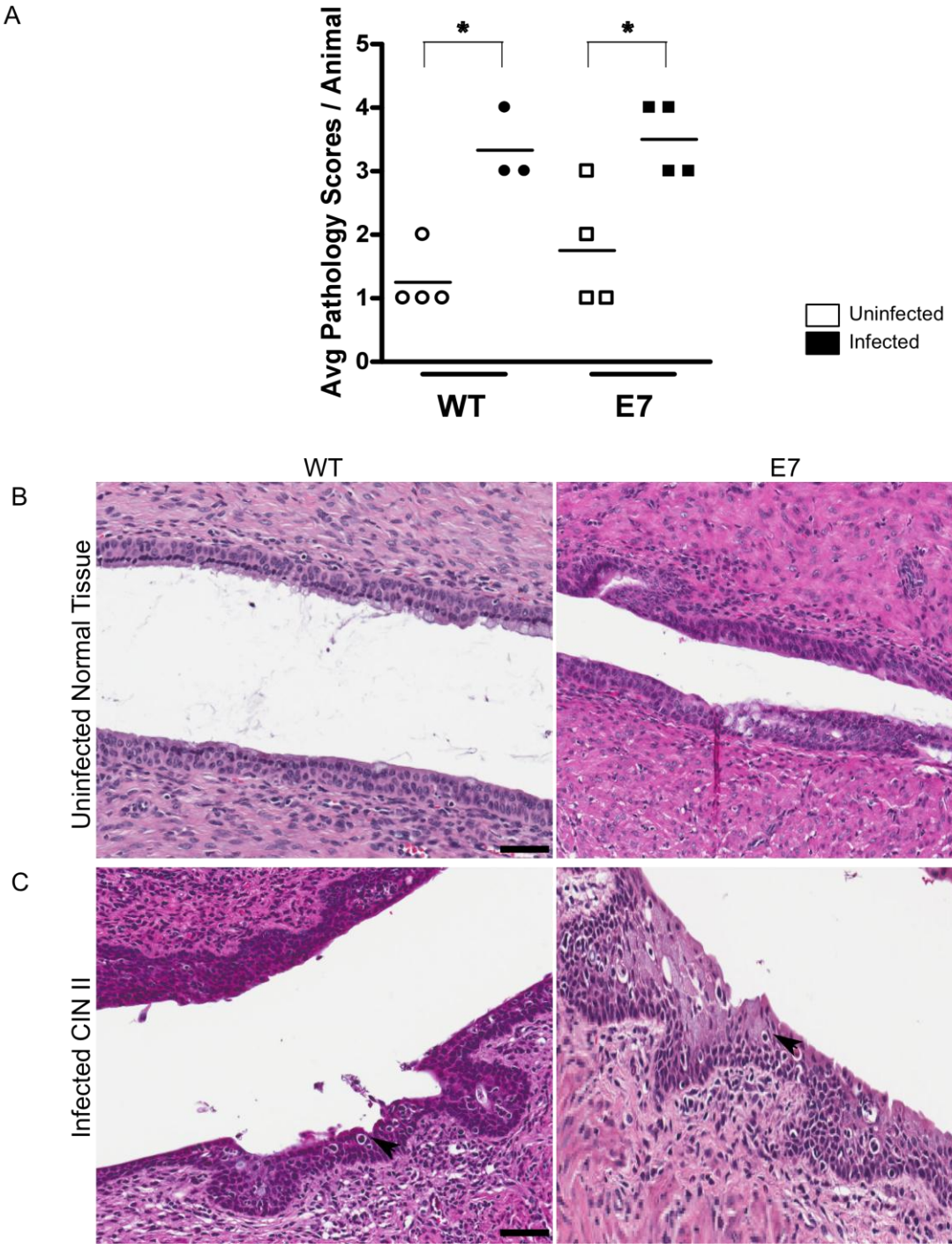
A
Avg Pathology Scores / Animal
0
1
2
3
4
5
*
*
WT
E7
Uninfected
Infected
WT
E7
B
Uninfected Normal Tissue
C
Infected CIN II

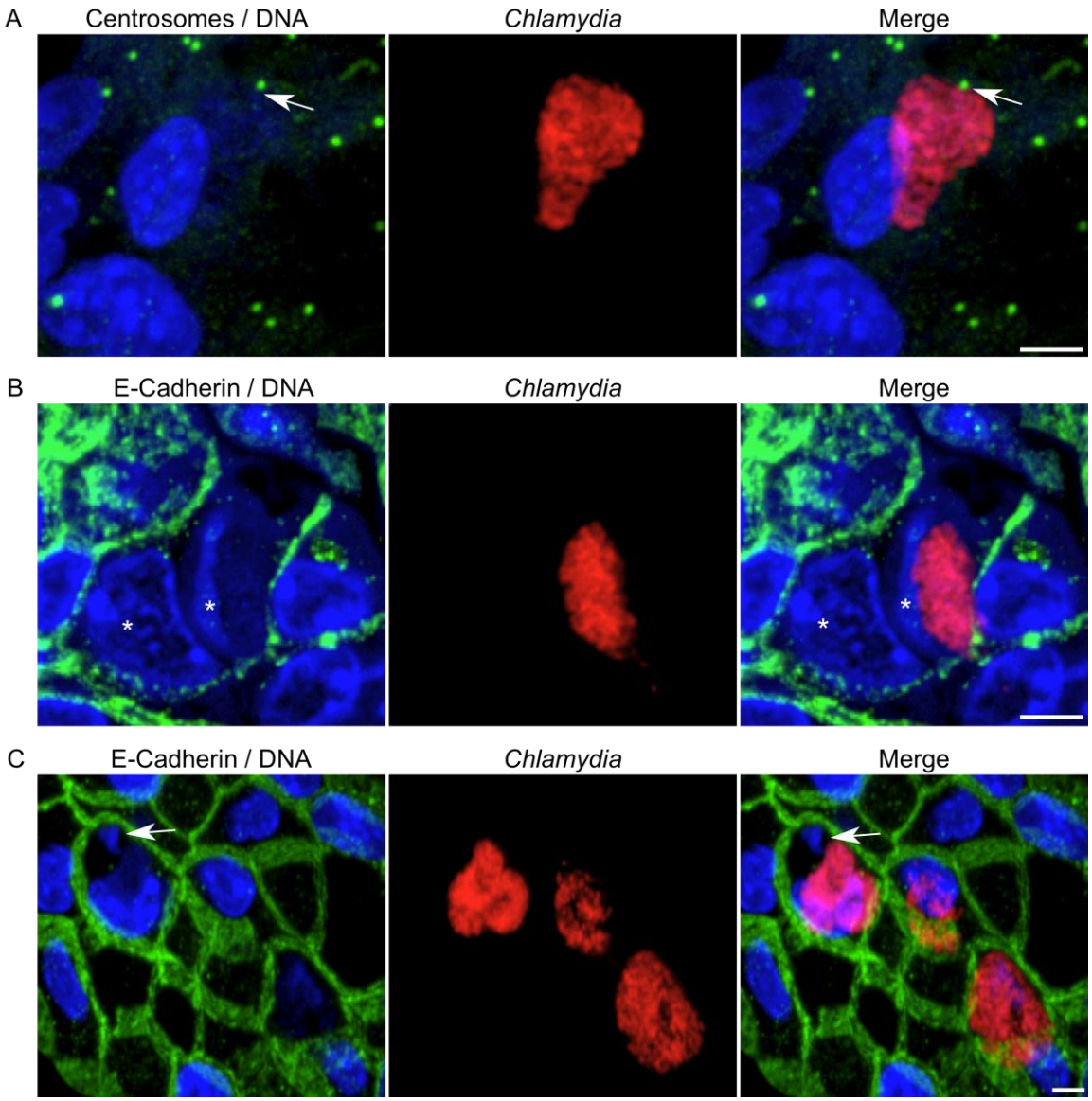


Figure 4-5. Evidence of centrosome mislocalization and genetic instability in infected animals. K14-HPV-E7 mice their wild-type littermates were infected on day 0 and boosted on day 3, and the animals were examined for phenotypic evidence of precancerous characteristics within the cervix. A) A 10μm thick tissue section from a wild-type mouse was stained for centrosomes (green), *Chlamydia* (red), and DNA (blue). The arrow indicates the centrosome is localized to the chlamydial inclusion. B) A K14-HPV-E7 tissue section was stained for E-Cadherin (green), *Chlamydia* (red), and DNA (blue). The stars denote two nuclei within the infected cell. The images in panel C are taken from wild-type tissue sections stained for E-cadherin (green), *Chlamydia* (red), and DNA (blue). The arrow indicates the formation of micronuclei. Scale bars, 5μm.

Table 4-1. Inclusion forming units (IFU) recovered from animals on day 1 postinfection

| Wild-type | IFU | K14-HPV-E7 | IFU |
|---|---|---|---|
| (N=3) | $1.28x10^7$ | (N=4) | $8.42x10^5$ |
| | $2.48x10^7$ | | $1.52x10^6$ |
| | $5.07x10^5$ | | $3.56x10^6$ |
| | | | $1.11x10^7$ |

Summary of live bacterial shedding from wild-type and K14-HPV-E7 infected mice.

# CHAPTER 5
# CONCLUSIONS AND FUTURE DIRECTIONS

The link between *Chlamydia trachomatis* and cervical cancer has been examined in several case-controlled and population based studies over the past decade and infection has been invariably associated with invasive cervical cancer (ICC), however a mechanism has yet to be established (Koskela et al., 2000; Anttila et al., 2001; Smith et al., 2002; Wallin et al., 2002; Matsumoto et al., 2003; Hinkula et al., 2004; Smith et al., 2004; Madeleine et al., 2007). In this study we show that a chlamydial infection is able to induce centrosome amplification and contribute to geometric centrosome spread. We demonstrate the physical separation of extra centrosomes in infected cells directly inhibits the host's ability to cluster extra centrosomes making it difficult to form bipolar spindles, leading to the formation of multipolar spindles. The presence of multipolar spindles and *Chlamydia's* ability to truncate mitosis and circumvent the spindle assembly checkpoint ultimately results in chromosomal instability and aneuploidy. During cell division the chlamydial inclusion can be partitioned so that one daughter cell inherits the inclusion, and the other daughter cell, while no longer infected, retains the chlamydial induced cellular defects (Campbell et al., 1989; Greene and Zhong, 2003). Grieshaber et al. has shown that even after infection is cured with antibiotics centrosome number defects persist, and previously infected cells develop micronuclei, a significant indicator of chromosomal instability (Grieshaber et al., 2006). Recent work to come out of our lab (Brown et al., 2012) demonstrated that chlamydial infection induces lagging chromosomes in anaphase, cytokinesis failure, and multinucleated cells, all of these contributing to aneuploidy and chromosomal instability.

Due to the phenotypic defects present in infected cells in culture we wanted to investigate *Chlamydia* infection *in vivo.* We showed for the first time that *Chlamydia* is able to infect actively replicating cells within the murine vaginal tract, an important finding as we have shown infection induces significant defects in replicating cells. We demonstrated that infection results in considerable increases in cell proliferation within the transformation zone of infected mice. We believe this induction in cell proliferation is an important first step in cancer progression. Infection also induced CIN II, or moderate cervical dysplasia, in wild-type mice and mice transgenic for the HPV oncoprotein E7. The development of CIN II is a particularly interesting finding as moderate dysplasia is a necessary precursor in the progression to invasive cervical cancer. In tissue sections from mice subjected to reinfection we observed evidence of centrosomes localized away from the nucleus and associated with the chlamydial inclusion, we observed multinucleated cells and the formation of micronuclei *in vivo*. Taken together these results suggest *Chlamydia* can act as a cofactor exacerbating HPV-induced cervical cancer. *Chlamydia* may also be considered an independent factor in cervical cancer development in cases in which reinfection has occurred.

More studies are necessary to fully elucidate the relationship between HPV infection, chlamydial infection, and cervical cancer formation. In the very immediate future we plan to infect primary cells in culture and test them for the ability to develop centrosome number defects, form multipolar spindles, and become multinucleated. We will also inhibit host cell protein synthesis with cylcoheximide and after infection examine centrosome numbers, spindle defects, and the presence of multinucleated cells in End1E6/E7 cells, COS-7, 3T3 and the aforementioned primary cells. These

experiments will facilitate our hypothesis that chlamydial infection needs to take place in a dividing cell population to induce cell defects and the expression of other oncogenes is not necessary. The short one week time period is not long enough to determine if chlamydial infection has any enduring effects on cervical cancer development. Further experiments should include a study of 9 months, as this is the time point all mice transgenic for HPV E7 develop invasive cervical cancer (Riley et al., 2003). To fully appreciate the relationship between HPV and *Chlamydia*, studies should also be done with mice transgenic for HPV E6 only, as well as the biologically relevant HPV E6-E7 mice. It is possible that the HPV oncoproteins E6 and E7 provide some necessary factors other than increased cell proliferation that we have not yet determined. We should also consider the age of the transgenic mice before infection, as we may see differences in cervical dysplasia progression in older mice compared to younger mice, as the older mice have encountered expression of the transgene for longer. We could infect transgenic mice at 6 months of age and determine the level of cervical dysplasia progression at 9 or 12 months of age to establish if the length of the expression of the transgene is a factor. Furthermore, the 3T3 soft agar model could be utilized in a tumor assay in which colonies formed in soft agar as a result of chlamydial transformation could be transferred to nude mice to determine if they are truly carcinogenic, as these studies would isolate the immune surveillance process from our hypothesized mechanism to transformation. To further understand the mechanisms by which *Chlamydia* induces these phenotypes we could perform microarray studies to examine host cell responses after chlamydial infection and determine which pathways may be important to cancer induction during infection. More studies need to be done to fully

understand the dynamic between chlamydial infection and HPV; however the results presented here provide new and important insight into *Chlamydia's* role in cervical cancer development.

LIST OF REFERENCES

Abdelrahman, Y.M., and Belland, R.J. (2005). The chlamydial developmental cycle. FEMS Microbiology Reviews *29*, 949-59.

Andersen, J.S., Wilkinson, C.J., Mayor, T., Mortensen, P., Nigg, E.A., and Mann, M. (2003). Proteomic characterization of the human centrosome by protein correlation profiling. Nature *426*, 570-4.

Anttila, T., Saikku, P., Koskela, P., Bloigu, A., Dillner, J., Ikäheimo, I., Jellum, E., Lehtinen, M., Lenner, P., Hakulinen, T., et al. (2001). Serotypes of Chlamydia trachomatis and risk for development of cervical squamous cell carcinoma. JAMA : The Journal Of The American Medical Association *285*, 47-51.

Autier, P., Coibion, M., Huet, F., and Grivegnee, A.R. (1996). Transformation zone location and intraepithelial neoplasia of the cervix uteri. British Journal Of Cancer *74*, 488-90.

Balsara, Z.R., Misaghi, S., Lafave, J.N., and Starnbach, M.N. (2006). Chlamydia trachomatis infection induces cleavage of the mitotic cyclin B1. Infection And Immunity *74*, 5602-8.

Basto, R., Brunk, K., Vinadogrova, T., Peel, N., Franz, A., Khodjakov, A., and Raff, J.W. (2008). Centrosome amplification can initiate tumorigenesis in flies. Cell *133*, 1032-42.

Belland, R., Ojcius, D.M., and Byrne, G.I. (2004). Focus: Chlamydia. Nature Reviews Microbiology *2*, 530-531.

Bettencourt-Dias, M., and Glover, D.M. (2007). Centrosome biogenesis and function: centrosomics brings new understanding. Nature Reviews. Molecular Cell Biology *8*, 451-63.

Boveri, T. (2008). Concerning the origin of malignant tumours by Theodor Boveri. Translated and annotated by Henry Harris. Journal Of Cell Science *121 Suppl 1*, 1-84.

Brake, T., and Lambert, P.F. (2005). Estrogen contributes to the onset, persistence, and malignant progression of cervical cancer in a human papillomavirus-transgenic mouse model. Proceedings Of The National Academy Of Sciences Of The United States Of America *102*, 2490-5.

Brinkley, B.R. (2001). Managing the centrosome numbers game: from chaos to stability in cancer cell division. Trends In Cell Biology *11*, 18-21.

Brown, H.M., Knowlton, A.E., and Grieshaber, S.S. (2012). Chlamydial Infection Induces Host Cytokinesis Failure at Abscission. Cellular Microbiology.

Campbell, S., Richmond, S.J., and Yates, P. (1989). The development of Chlamydia trachomatis inclusions within the host eukaryotic cell during interphase and mitosis. Journal Of General Microbiology *135*, 1153-65.

Carabeo, R.A., Mead, D.J., and Hackstadt, T. (2003). Golgi-dependent transport of cholesterol to the Chlamydia trachomatis inclusion. Proceedings Of The National Academy Of Sciences Of The United States Of America *100*, 6771-6.

Cates, W., and Wasserheit, J.N. (1991). Genital chlamydial infections: epidemiology and reproductive sequelae. American Journal Of Obstetrics And Gynecology *164*, 1771-81.

Chellas-Géry, B., Linton, C.N., and Fields, K.A. (2007). Human GCIP interacts with CT847, a novel Chlamydia trachomatis type III secretion substrate, and is degraded in a tissue-culture infection model. Cellular Microbiology *9*, 2417-30.

Chi, Y., and Jeang, K. (2007). Aneuploidy and cancer. Journal Of Cellular Biochemistry *102*, 531-8.

Clifton, D.R., Fields, K.A., Grieshaber, S.S., Dooley, C.A., Fischer, E.R., Mead, D.J., Carabeo, R.A., and Hackstadt, T. (2004). A chlamydial type III translocated protein is tyrosine-phosphorylated at the site of entry and associated with recruitment of actin. Proceedings Of The National Academy Of Sciences Of The United States Of America *101*, 10166-71.

Cohen, C.R., and Brunham, R.C. (1999). Pathogenesis of Chlamydia induced pelvic inflammatory disease. Sexually Transmitted Infections *75*, 21-4.

Cook, J.A. (2008). Eliminating blinding trachoma. The New England Journal Of Medicine *358*, 1777-9.

Cotter, T.W., Meng, Q., Shen, Z.L., Zhang, Y.X., Su, H., and Caldwell, H.D. (1995). Protective efficacy of major outer membrane protein-specific immunoglobulin A (IgA) and IgG monoclonal antibodies in a murine model of Chlamydia trachomatis genital tract infection. Infection And Immunity *63*, 4704-14.

Da Barros, N.K., Costa, M.C., Alves, R.R., Villa, L.L., Derchain, S.F., Zeferino, L.C., Carneiro, dos, M.A., and Rabelo-Santos, S.H. (2012). Association of HPV infection and Chlamydia trachomatis seropositivity in cases of cervical neoplasia in Midwest Brazil. Journal Of Medical Virology *84*, 1143-50.

DiPaolo, J.A., Donovan, P., and Nelson, R. (1969). Quantitative studies of in vitro transformation by chemical carcinogens. Journal Of The National Cancer Institute *42*, 867-74.

Duensing, A., Chin, A., Wang, L., Kuan, S., and Duensing, S. (2008). Analysis of centrosome overduplication in correlation to cell division errors in high-risk human papillomavirus (HPV)-associated anal neoplasms. Virology *372*, 157-64.

Duensing, S., Duensing, A., Flores, E.R., Do A, Lambert, P.F., and Münger, K. (2001). Centrosome abnormalities and genomic instability by episomal expression of human papillomavirus type 16 in raft cultures of human keratinocytes. Journal Of Virology *75*, 7712-6.

Elson, D.A., Riley, R.R., Lacey, A., Thordarson, G., Talamantes, F.J., and Arbeit, J.M. (2000). Sensitivity of the cervical transformation zone to estrogen-induced squamous carcinogenesis. Cancer Research *60*, 1267-75.

Fenech, M., Kirsch-Volders, M., Natarajan, A.T., Surralles, J., Crott, J.W., Parry, J., Norppa, H., Eastmond, D.A., Tucker, J.D., and Thomas, P. (2011). Molecular mechanisms of micronucleus, nucleoplasmic bridge and nuclear bud formation in mammalian and human cells. Mutagenesis *26*, 125-32.

Fichorova, R.N., Rheinwald, J.G., and Anderson, D.J. (1997). Generation of papillomavirus-immortalized cell lines from normal human ectocervical, endocervical, and vaginal epithelium that maintain expression of tissue-specific differentiation proteins. Biology Of Reproduction *57*, 847-55.

Frazer, I.H. (2004). Prevention of cervical cancer through papillomavirus vaccination. Nature Reviews. Immunology *4*, 46-54.

Fukasawa, K. (2007). Oncogenes and tumour suppressors take on centrosomes. Nature Reviews. Cancer *7*, 911-24.

Gaetz, J., and Kapoor, T.M. (2004). Dynein/dynactin regulate metaphase spindle length by targeting depolymerizing activities to spindle poles. The Journal Of Cell Biology *166*, 465-71.

Ganem, N.J., Godinho, S.A., and Pellman, D. (2009). A mechanism linking extra centrosomes to chromosomal instability. Nature *460*, 278-82.

Garland, S.M., Lees, M.I., and Skurrie, I.J. (1990). Chlamydia trachomatis--role in tubal infertility. The Australian &Amp;Amp; New Zealand Journal Of Obstetrics &Amp;Amp; Gynaecology *30*, 83-6.

Gisselsson, D. (2008). Classification of chromosome segregation errors in cancer. Chromosoma *117*, 511-9.

Gluzman, Y. (1981). SV40-transformed simian cells support the replication of early SV40 mutants. Cell *23*, 175-82.

Greene, W., Xiao, Y., Huang, Y., McClarty, G., and Zhong, G. (2004). Chlamydia-infected cells continue to undergo mitosis and resist induction of apoptosis. Infection And Immunity *72*, 451-60.

Greene, W., and Zhong, G. (2003). Inhibition of host cell cytokinesis by Chlamydia trachomatis infection. The Journal Of Infection *47*, 45-51.

Grieshaber, S.S., Grieshaber, N.A., Miller, N., and Hackstadt, T. (2006). Chlamydia trachomatis causes centrosomal defects resulting in chromosomal segregation abnormalities. Traffic (Copenhagen, Denmark) *7*, 940-9.

Grieshaber, S.S., Grieshaber, N.A., and Hackstadt, T. (2003). Chlamydia trachomatis uses host cell dynein to traffic to the microtubule-organizing center in a p50 dynamitin-independent process. Journal Of Cell Science *116*, 3793-802.

Guderian, A.M., and Trobough, G.E. (1986). Residues of pelvic inflammatory disease in intrauterine device users: a result of the intrauterine device or Chlamydia trachomatis infection? American Journal Of Obstetrics And Gynecology *154*, 497-503.

Hackstadt, T., Scidmore, M.A., and Rockey, D.D. (1995). Lipid metabolism in Chlamydia trachomatis-infected cells: directed trafficking of Golgi-derived sphingolipids to the chlamydial inclusion. Proceedings Of The National Academy Of Sciences Of The United States Of America *92*, 4877-81.

Handsfield, H.H. (1983). Recent developments in gonorrhea and pelvic inflammatory disease. Journal Of Medicine *14*, 281-305.

Helfand, B.T., Mikami, A., Vallee, R.B., and Goldman, R.D. (2002). A requirement for cytoplasmic dynein and dynactin in intermediate filament network assembly and organization. The Journal Of Cell Biology *157*, 795-806.

Henry-Suchet, J., Utzmann, C., de Brux, J., Ardoin, P., and Catalan, F. (1987). Microbiologic study of chronic inflammation associated with tubal factor infertility: role of Chlamydia trachomatis. Fertility And Sterility *47*, 274-7.

Herber, R., Liem, A., Pitot, H., and Lambert, P.F. (1996). Squamous epithelial hyperplasia and carcinoma in mice transgenic for the human papillomavirus type 16 E7 oncogene. Journal Of Virology *70*, 1873-81.

Hinkula, M., Pukkala, E., Kyyrönen, P., Laukkanen, P., Koskela, P., Paavonen, J., Lehtinen, M., and Kauppila, A. (2004). A population-based study on the risk of cervical cancer and cervical intraepithelial neoplasia among grand multiparous women in Finland. British Journal Of Cancer *90*, 1025-9.

Ho, G.Y., Bierman, R., Beardsley, L., Chang, C.J., and Burk, R.D. (1998). Natural history of cervicovaginal papillomavirus infection in young women. The New England Journal Of Medicine *338*, 423-8.

Howard, L., Orenstein, N.S., and King, N.W. (1974). Purification on renografin density gradients of Chlamydia trachomatis grown in the yolk sac of eggs. Applied Microbiology *27*, 102-6.

Howe, D., and Heinzen, R.A. (2006). Coxiella burnetii inhabits a cholesterol-rich vacuole and influences cellular cholesterol metabolism. Cellular Microbiology *8*, 496-507.

Johnson, K.A., Tan, M., and Sütterlin, C. (2009). Centrosome abnormalities during a Chlamydia trachomatis infection are caused by dysregulation of the normal duplication pathway. Cellular Microbiology *11*, 1064-73.

Kelver, M.E., and Nagamani, M. (1989). Chlamydial serology in women with tubal infertility. International Journal Of Fertility *34*, 42-5.

Kirsch-Volders, M., Elhajouji, A., Cundari, E., and van Hummelen, P. (1997). The in vitro micronucleus test: a multi-endpoint assay to detect simultaneously mitotic delay, apoptosis, chromosome breakage, chromosome loss and non-disjunction. Mutation Research *392*, 19-30.

Kiviat, N.B., Paavonen, J.A., Brockway, J., Critchlow, C.W., Brunham, R.C., Stevens, C.E., Stamm, W.E., Kuo, C.C., DeRouen, T., and Holmes, K.K. (1985). Cytologic manifestations of cervical and vaginal infections. I. Epithelial and inflammatory cellular changes. JAMA : The Journal Of The American Medical Association *253*, 989-96.

Knowlton, A.E., Brown, H.M., Richards, T.S., Andreolas, L.A., Patel, R.K., and Grieshaber, S.S. (2011). Chlamydia trachomatis infection causes mitotic spindle pole defects independently from its effects on centrosome amplification. Traffic (Copenhagen, Denmark) *12*, 854-66.

Koskela, P., Anttila, T., Bjørge, T., Brunsvig, A., Dillner, J., Hakama, M., Hakulinen, T., Jellum, E., Lehtinen, M., Lenner, P., et al. (2000). Chlamydia trachomatis infection as a risk factor for invasive cervical cancer. International Journal Of Cancer. Journal International Du Cancer *85*, 35-9.

Lasne, C., Gentil, A., and Chouroulinkov, I. (1974). Two-stage malignant transformation of rat fibroblasts in tissue culture. Nature *247*, 490-1.

Lax, A.J., and Thomas, W. (2002). How bacteria could cause cancer: one step at a time. Trends In Microbiology *10*, 293-9.

Leppert, P.C. (2012). Tissue remodeling in the female reproductive tract--a complex process becomes more complex: the role of Hox genes. Biology Of Reproduction *86*, 98.

Lingle, W.L., Barrett, S.L., Negron, V.C., D'Assoro, A.B., Boeneman, K., Liu, W., Whitehead, C.M., Reynolds, C., and Salisbury, J.L. (2002). Centrosome amplification drives chromosomal instability in breast tumor development. Proceedings Of The National Academy Of Sciences Of The United States Of America *99*, 1978-83.

Madeleine, M.M., Anttila, T., Schwartz, S.M., Saikku, P., Leinonen, M., Carter, J.J., Wurscher, M., Johnson, L.G., Galloway, D.A., and Daling, J.R. (2007). Risk of cervical cancer associated with Chlamydia trachomatis antibodies by histology, HPV type and HPV cofactors. International Journal Of Cancer. Journal International Du Cancer *120*, 650-5.

Martin, D.H. (1990). Chlamydial infections. The Medical Clinics Of North America *74*, 1367-87.

Matsumoto, K., Yasugi, T., Oki, A., Hoshiai, H., Taketani, Y., Kawana, T., and Yoshikawa, H. (2003). Are smoking and chlamydial infection risk factors for CIN? Different results after adjustment for HPV DNA and antibodies. British Journal Of Cancer *89*, 831-3.

Merdes, A., Ramyar, K., Vechio, J.D., and Cleveland, D.W. (1996). A complex of NuMA and cytoplasmic dynein is essential for mitotic spindle assembly. Cell *87*, 447-58.

Miller, W.C., Ford, C.A., Morris, M., Handcock, M.S., Schmitz, J.L., Hobbs, M.M., Cohen, M.S., Harris, K.M., and Udry, J.R. (2004). Prevalence of chlamydial and gonococcal infections among young adults in the United States. JAMA : The Journal Of The American Medical Association *291*, 2229-36.

Morrison, S.G., Farris, C.M., Sturdevant, G.L., Whitmire, W.M., and Morrison, R.P. (2011). Murine Chlamydia trachomatis genital infection is unaltered by depletion of CD4+ T cells and diminished adaptive immunity. The Journal Of Infectious Diseases *203*, 1120-8.

Moulder, J.W. (1991). Interaction of chlamydiae and host cells in vitro. Microbiological Reviews *55*, 143-90.

Musacchio, A., and Salmon, E.D. (2007). The spindle-assembly checkpoint in space and time. Nature Reviews. Molecular Cell Biology *8*, 379-93.

Muñoz, N., Bosch, F.X., de Sanjosé, S., Herrero, R., Castellsagué, X., Shah, K.V., Snijders, P.J., and Meijer, C.J. (2003). Epidemiologic classification of human papillomavirus types associated with cervical cancer. The New England Journal Of Medicine *348*, 518-27.

Muñoz, N., Castellsagué, X., de González, A.B., and Gissmann, L. (2006). Chapter 1: HPV in the etiology of human cancer. Vaccine *24 Suppl 3*, S3/1-10.

Münger, K., Phelps, W.C., Bubb, V., Howley, P.M., and Schlegel, R. (1989). The E6 and E7 genes of the human papillomavirus type 16 together are necessary and sufficient for transformation of primary human keratinocytes. Journal Of Virology *63*, 4417-21.

Münger, K., and Howley, P.M. (2002). Human papillomavirus immortalization and transformation functions. Virus Research *89*, 213-28.

Narisawa-Saito, M., and Kiyono, T. (2007). Basic mechanisms of high-risk human papillomavirus-induced carcinogenesis: roles of E6 and E7 proteins. Cancer Science *98*, 1505-11.

Nguyen, C.L., McLaughlin-Drubin, M.E., and Münger, K. (2008). Delocalization of the microtubule motor Dynein from mitotic spindles by the human papillomavirus E7 oncoprotein is not sufficient for induction of multipolar mitoses. Cancer Research *68*, 8715-22.

Nguyen, C.L., and Münger, K. (2009). Human papillomavirus E7 protein deregulates mitosis via an association with nuclear mitotic apparatus protein 1. Journal Of Virology *83*, 1700-7.

Nigg, E.A. (2002). Centrosome aberrations: cause or consequence of cancer progression? Nature Reviews. Cancer *2*, 815-25.

Nigg, E.A. (2006). Origins and consequences of centrosome aberrations in human cancers. International Journal Of Cancer. Journal International Du Cancer *119*, 2717-23.

Nigg, E.A. (2007). Centrosome duplication: of rules and licenses. Trends In Cell Biology *17*, 215-21.

Paschen, S.A., Christian, J.G., Vier, J., Schmidt, F., Walch, A., Ojcius, D.M., and Häcker, G. (2008). Cytopathicity of Chlamydia is largely reproduced by expression of a single chlamydial protease. The Journal Of Cell Biology *182*, 117-27.

Patton, D.L., Landers, D.V., and Schachter, J. (1989). Experimental Chlamydia trachomatis salpingitis in mice: initial studies on the characterization of the leukocyte response to chlamydial infection. The Journal Of Infectious Diseases *159*, 1105-10.

Peters, J. (2006). The anaphase promoting complex/cyclosome: a machine designed to destroy. Nature Reviews. Molecular Cell Biology *7*, 644-56.

Piel, M., Meyer, P., Khodjakov, A., Rieder, C.L., and Bornens, M. (2000). The respective contributions of the mother and daughter centrioles to centrosome activity and behavior in vertebrate cells. The Journal Of Cell Biology *149*, 317-30.

Pihan, G., Wallace, J., and Zhou, Y. (2003). Centrosome abnormalities and chromosome instability occur together in pre-invasive carcinomas. Cancer Research.

Pihan, G.A., Purohit, A., Wallace, J., Knecht, H., Woda, B., Quesenberry, P., and Doxsey, S.J. (1998). Centrosome defects and genetic instability in malignant tumors. Cancer Research *58*, 3974-85.

Quintyne, N.J., Reing, J.E., Hoffelder, D.R., Gollin, S.M., and Saunders, W.S. (2005). Spindle multipolarity is prevented by centrosomal clustering. Science (New York, N.Y.) *307*, 127-9.

Read, T.D., Brunham, R.C., Shen, C., Gill, S.R., Heidelberg, J.F., White, O., Hickey, E.K., Peterson, J., Utterback, T., Berry, K., et al. (2000). Genome sequences of Chlamydia trachomatis MoPn and Chlamydia pneumoniae AR39. Nucleic Acids Research *28*, 1397-406.

Rebacz, B., Larsen, T.O., Clausen, M.H., Rønnest, M.H., Löffler, H., Ho, A.D., and Krämer, A. (2007). Identification of griseofulvin as an inhibitor of centrosomal clustering in a phenotype-based screen. Cancer Research *67*, 6342-50.

Reniers, J., Collet, M., Frost, Leclerc, A., Ivanoff, B., and Méheus, A. (1989). Chlamydial antibodies and tubal infertility. International Journal Of Epidemiology *18*, 261-3.

Riley, R.R., Duensing, S., Brake, T., Münger, K., Lambert, P.F., and Arbeit, J.M. (2003). Dissection of human papillomavirus E6 and E7 function in transgenic mouse models of cervical carcinogenesis. Cancer Research *63*, 4862-71.

Ring, D., Hubble, R., and Kirschner, M. (1982). Mitosis in a cell with multiple centrioles. The Journal Of Cell Biology *94*, 549-56.

Sakaue-Sawano, A., Kurokawa, H., Morimura, T., Hanyu, A., Hama, H., Osawa, H., Kashiwagi, S., Fukami, K., Miyata, T., Miyoshi, H., et al. (2008). Visualizing spatiotemporal dynamics of multicellular cell-cycle progression. Cell *132*, 487-98.

Salic, A., and Mitchison, T.J. (2008). A chemical method for fast and sensitive detection of DNA synthesis in vivo. Proceedings Of The National Academy Of Sciences Of The United States Of America *105*, 2415-20.

Saunders, W. (2005). Centrosomal amplification and spindle multipolarity in cancer cells. Seminars In Cancer Biology *15*, 25-32.

Schachter, J. (1999). Infection and disease epidemiology. In Chlamydia: Intracellular Biology, Pathogenesis, and Immunity, R.S. Stephens, ed. (Washington, DC: ASM Press) pp. 139-169.

Schwarz, E., Freese, U.K., Gissmann, L., Mayer, W., Roggenbuck, B., Stremlau, A., and Hausen, H.Z. (1985). Structure and transcription of human papillomavirus sequences in cervical carcinoma cells. Nature *314*, 111-4.

Shah, A.A., Schripsema, J.H., Imtiaz, M.T., Sigar, I.M., Kasimos, J., Matos, P.G., Inouye, S., and Ramsey, K.H. (2005). Histopathologic changes related to fibrotic oviduct occlusion after genital tract infection of mice with Chlamydia muridarum. Sexually Transmitted Diseases *32*, 49-56.

Shin, S.I., Freedman, V.H., Risser, R., and Pollack, R. (1975). Tumorigenicity of virus-transformed cells in nude mice is correlated specifically with anchorage independent growth in vitro. Proceedings Of The National Academy Of Sciences Of The United States Of America *72*, 4435-9.

Sluder, G. (2004). The good, the bad and the ugly: the practical consequences of centrosome amplification. Current Opinion In Cell Biology.

Smith J.S., Bosetti, C., Muñoz, N., Herrero, R., Bosch, F.X., Eluf-Neto, J., Meijer, C.J., Van Den Brule, A.J., Franceshci, S., Peeling, R.W., et al. (2004). Chlamydia trachomatis and invasive cervical cancer: a pooled analysis of the IARC multicentric case-control study. International Journal Of Cancer. Journal International Du Cancer *111*, 431-9.

Smith, J.S., Muñoz, N., Herrero, R., Eluf-Neto, J., Ngelangel, C., Franceschi, S., Bosch, F.X., Walboomers, J.M., and Peeling, R.W. (2002). Evidence for Chlamydia trachomatis as a human papillomavirus cofactor in the etiology of invasive cervical cancer in Brazil and the Philippines. The Journal Of Infectious Diseases *185*, 324-31.

Steenbergen, R.D., de Wilde, J., Wilting, S.M., Brink, A.A., Snijders, P.J., and Meijer, C.J. (2005). HPV-mediated transformation of the anogenital tract. Journal Of Clinical Virology : The Official Publication Of The Pan American Society For Clinical Virology *32 Suppl 1*, S25-33.

Stephens, R.S., Kalman, S., Lammel, C., Fan, J., Marathe, R., Aravind, L., Mitchell, W., Olinger, L., Tatusov, R.L., Zhao, Q., et al. (1998). Genome sequence of an obligate intracellular pathogen of humans: Chlamydia trachomatis. Science (New York, N.Y.) *282*, 754-9.

Todaro, G.J., and Green, H. (1963). Quantitative studies of the growth of mouse embryo cells in culture and their development into established lines. The Journal Of Cell Biology *17*, 299-313.

Walboomers, J.M., Jacobs, M.V., Manos, M.M., Bosch, F.X., Kummer, J.A., Shah, K.V., Snijders, P.J., Peto, J., Meijer, C.J., and Muñoz, N. (1999). Human papillomavirus is a necessary cause of invasive cervical cancer worldwide. The Journal Of Pathology *189*, 12-9.

Wallin, K., Wiklund, F., Luostarinen, T., Angström, T., Anttila, T., Bergman, F., Hallmans, G., Ikäheimo, I., Koskela, P., Lehtinen, M., et al. (2002). A population-based prospective study of Chlamydia trachomatis infection and cervical carcinoma. International Journal Of Cancer. Journal International Du Cancer *101*, 371-4.

Wheeler, C.M. (2008). Natural history of human papillomavirus infections, cytologic and histologic abnormalities, and cancer. Obstetrics And Gynecology Clinics Of North America *35*, 519-36; vii.

Woodman, C.B., Collins, S.I., and Young, L.S. (2007). The natural history of cervical HPV infection: unresolved issues. Nature Reviews. Cancer *7*, 11-22.

Yoheved, Sachs, and Berwald, L. (2004). IN VITRO Cell Transformation with Chemical Carcinogens. Nature 1963 *200*, 1182-1184.

Zhong, G., Fan, P., Ji, H., Dong, F., and Huang, Y. (2001). Identification of a chlamydial protease-like activity factor responsible for the degradation of host transcription factors. The Journal Of Experimental Medicine *193*, 935-42.

Zyss, D., and Gergely, F. (2009). Centrosome function in cancer: guilty or innocent? Trends In Cell Biology *19*, 334-46.

zur Hausen, H. (1996). Papillomavirus infections--a major cause of human cancers. Biochimica Et Biophysica Acta *1288*, F55-78.

zur Hausen, H. (2002). Papillomaviruses and cancer: from basic studies to clinical application. Nature Reviews. Cancer *2*, 342-50.

zur Hausen, H. (2009). Papillomaviruses in the causation of human cancers - a brief historical account. Virology *384*, 260-5.

WHO (2001). Global Prevalence and Incidence of Selected Curable Sexually Transmitted Infections: Overview and Estimates. World Health Organizaion, Geneva (2001). 1-50.

# BIOGRAPHICAL SKETCH

Andrea was born to Greg and Nancy Knowlton in Boynton Beach, Florida. During her childhood Andrea was always curious about the world, but when her little sister Amy was born with Down syndrome, Andrea's curiosity focused on medical science. Andrea started taking advanced science classes in high school, and when she started college at the University of Florida began a microbiology and cell science track. Andrea's initial intent was to attend medical school and focus on genetic conditions like Down syndrome. This was until her first microbiology class and accompanying lab. Andrea loved learning about microbiology and talking to the graduate assistants about their projects. After college she worked as a lab technician in the College of Dentistry for a year before she was accepted into the Interdisciplinary Program at UF. Andrea began research on the pathogenesis of *Chlamydia trachomatis* under her mentor Dr. Scott Grieshaber, and received her Ph.D. in the summer of 2012. Andrea hopes to have a career that will benefit the lives and public health of women.